„BABEȘ-BOLYAI" UNIVERSITY, CLUJ-NAPOCA
F A C U L T Y O F G E O G R A P H Y
DOCTORAL SCHOOL OF GEOGRAPHY

PhD THESIS
SUMMARY

THE RECONSTRUCTION OF SNOW AVALANCHE ACTIVITY FROM THE PARÂNG MOUNTAINS

Scientific coordinator,
prof. univ. dr. Dănuț PETREA

PhD Student,
Flaviu MESEȘAN

2020

TABLE OF CONTENTS

KEYWORDS

- Dendrogeomorphology
- Snow avalanche
- Parâng Mountains
- Remote sensing
- GIS

INTRODUCTION

The present study aims at analysing the temporal and spatial occurrence of the snow avalanches which have previously formed in the Parâng Mountains. Because the activity of avalanches is not monitored in this area, the tree rings of annual growth represent one of the most important sources of data related to these geomorphological processes.

The general purpose of this study is the analysis of the temporal and spatial occurrence of past snow avalanches which took place on the surface of the Parâng Mountains. This will be materialised through the following objectives:

1. The identification of the frequency, the spatial extension and the recurrence period of snow avalanches for each avalanche path selected as case study;
2. The identification of the spatial extension of snow avalanches in one winter with the help of satellite images;
3. The identification of the meteorological conditions necessary for triggering snow avalanches.

The original elements of this study are presented in the following section. (i) A new procedure has been developed for centralising the growth anomalies which are present in the sample trees by applying personalised formulae implemented in Microsoft Excel. (ii) A new, automatic algorithm was proposed for calculating the return period of snow avalanches in an avalanche path using the location and the growth anomalies of the sample trees. (iii) A correlation was made between the growth anomalies of sample trees due to snow avalanches and satellite images. It was demonstrated that both sets of data can show the impact of snow avalanches. (iv) Using statistical analysis, a set of necessary meteorological conditions was determined for the triggering of the major snow avalanches from the Parâng Mountains.

I wish to thank to the administrators of the Parâng Site ROSCI 0188 for granting the sampling of the trees. I also want to thank to Lecturer PhD Olimpiu Pop and Associate Professor PhD Iulian Holobâcă for the assistance and support in attaining and analysing the data used in this study. My gratitude also goes to the colleagues from the Dendrochronology Laboratory of the Faculty of Geography (UBB) and to my father, for his availability to accompany me on the field, for his help and his opinions.

Last, but not least, I want to express my gratitude towards Professor PhD Dănuț Petrea for the trust he has granted me during all these years, for his patience, his encouragement and the advice and ideas offered for the accomplishment of this study.

1. THE GEOGRAPHIC INDIVIDUALITY OF THE PARÂNG MOUNTAINS

1.1. The location of the Parâng Mountains

The Parâng Mountains are a part of the Southern Carpathians, where a mountain group bears their name: The Group of the Parâng Mountains, located between the Olt Valley and the Jiu Valley. In this group, the Parâng Mountains form an orographic node situated in its south-western edge (Fig. 1).

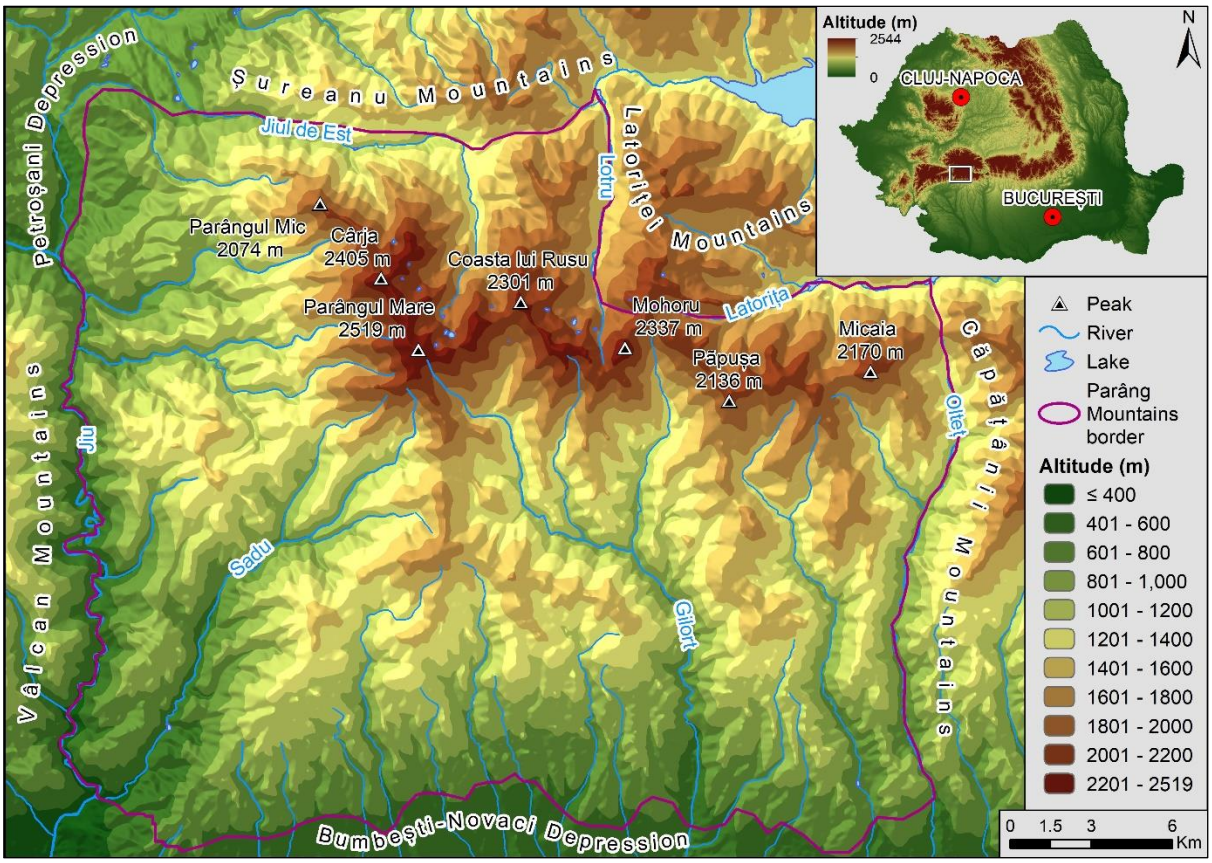

Fig. 1 The location and the limits of the Parâng Mountains

The surface of the Parâng Mountains is 795 km^2, out of which less than 150 km^2 are fount at altitudes above 1600 meters. Inside this area, there are the starting zones of all avalanche paths from this mountain unit. Out of the total surface of these mountains, approximately 37 km^2 are found at altitudes above 2000 m.

1.2. General geographic characteristics of the Parâng Mountains

The Parâng Mountains represent the highest mountain massif from the mountain group with the same name from the Southern Carpathians. The north-south axis of this mountain unit has a length of approximately 33 km, and the east-west axis approximately 32 km (Bud, 2008).

Due to its hard rock substratum, the topography of the Parâng Mountains is characterised by massivity, high altitudes (it represents the second highest mountain group from Romania after the Făgăraș Mountains), the existence of relict landforms which are very well preserved (erosion surfaces, glacial landforms), the presence of a typical glacial morphology (glacial valleys and ridges), the presence of an uninterrupted ridge with altitudes over 2000 m (Bud, 2008), massive, rounded ridges, separated by deep valleys. The general aspect of the Parâng Mountains is of a stepped pyramid with a central ridge in the shape of the letter „L" (Badea et al., 2001).

The highest sector of the Parâng Mountains, with altitudes over 2200 m, forms a strip along the main ridge between the Cârja and Mohoru Peaks. From it, secondary ridges radiate towards north and south among which, sometimes, glacial cirques intercalate (Iancu, 1970).

The main ridge of the Parâng Mountains has an asymmetrical transversal profile with steeper slopes towards north. From the south, these mountains have the aspect of monotonous, well forested ridges. On the other hand, when seen from the north, they almost have an alpine aspect. Due to the asymmetry of this ridge, the largest glacial cirques are located on the northern slope (Dragu et al., 1987).

The main genetic types of landforms on the alpine level of the Parâng Mountains are the glacial, periglacial and aeolian landforms. The glacial topography is formed by the action of glaciers and snow. The main forms of erosion are glacial cirques and valleys and the main depositional landforms are moraines, fluvio-glacial deposits, polished rocks, fields of blocks etc. (Coteț, 1973). At present, these landforms are relict and are being modelled by other geomorphological processes (Iancu, 1970). The periglacial topography was formed outside the areas affected by glaciation and is characterised by landforms like rock glaciers, polygonal soils etc. In the aeolian topography, the wind models erosion remnants and snow accumulation.

In the Parâng Mountains, the surface of the areas with a potential for snow avalanche occurrence is of 49.9 km^2, representing 6.8% of the massif surface. The largest part of this surface is located on the southern slope. The anthropic elements present in this area are represented by tourist paths, sheepfolds and the Transalpina road (Săndulache, 2009). The main glacial complexes which were identified in the Parâng Mountains can be seen in Fig. 2.

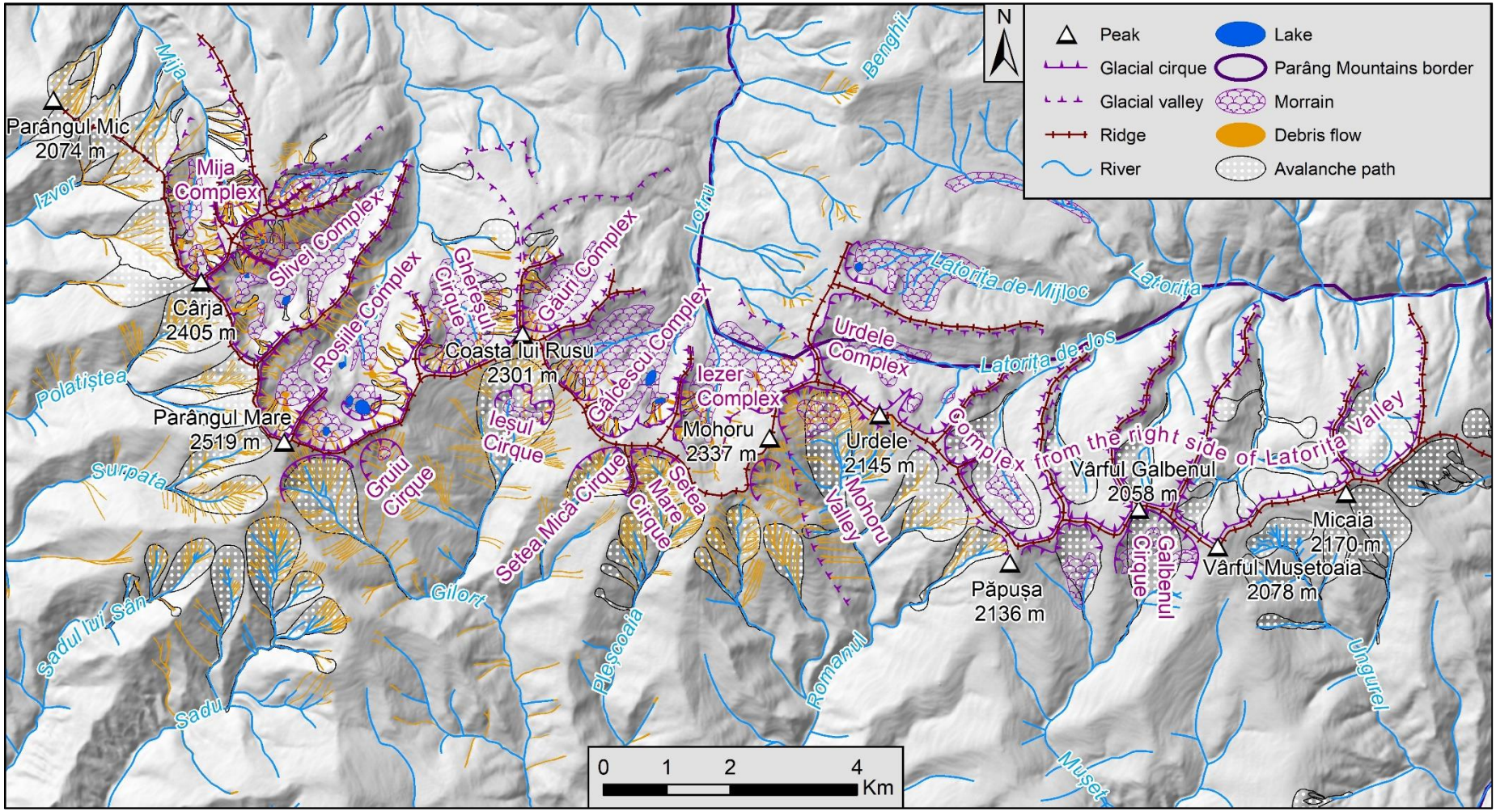

Fig. 2 Alpine area of Parâng Mountains – geomorphological sketch

2. PREVIOUS RESEARCH ON THE PARÂNG MOUNTAINS AND THE PRESENT STAGE OF SNOW AVALANCHE STUDY THROUGH THE DENDROGEOMORPHOLOGIC METHOD

The first scientific research of the Parâng Mountains dates from the end of the 19th century and is represented by geologic investigations of this area. The beginning of geographic knowledge related to the Parâng Mountains is owed to the geographer Emmanuel de Martonne who offered them a significant role in his PhD thesis „The Transylvanian Alps" (Martonne, 1907). Eventually, studies of the Parâng Mountains were written by I. Ichim, Gh. Niculescu and other researchers like the faculty members of the Faculty of Geography from the West University of Timișoara.

Until now, the Parâng Mountains have represented the study area of three PhD theses. The first was defended by Silvia Iancu in 1970 and it was entitled „*Masivul Parâng. Studiu de geomorfologie*" (*The Parâng Massif. A geomorphological study*). The next two were defended in 2009, by Cătălina Săndulache („*Hazarde și riscuri naturale în Munții Parâng*" / *Natural hazards and risks in the Parâng Mountains*) and Maria Bud („*Ecoturismul în grupa montană Parâng*" / *Ecotourism in the Parâng mountain unit*), respectively.

The initiator of dendrochronology is Andrew Ellicott Douglass (1867-1962), a researcher at the astronomical observatory from Flagstaff – Arizona. He noticed similarities between the width of tree rings even for trees which were located at large distances from each other, setting the basis for crossdating (Cook and Kairiukstis, 1992). The first applications of this principle were in archaeology and enabled the dating of some Aztec ruins (Douglas, 1921).

A significant contribution to the beginnings of dendrochronology was represented by the study *Dendrochronological interpretation of geomorphic processes*, published by the Finn Jurko Alestalo (1971). The notion of "dendrogeomorphology" is used for the first time in this paper.

At present, in Romania, research in this field is performed in the laboratories of dendrochronology from the West University (Timișoara), "Ștefan cel Mare" University (Suceava), Bucharest University (București), The institute of Wood Research (Câmpulung Moldovenesc) and the University of "Transylvania" (Brașov). In the Faculty of Geography from the "Babeș-Bolyai" University of Cluj-Napoca the studies of dendrochronology are performed in the Laboratory of Dendrogeomorphology which is part of the Research Center of Geographical Hazards and Risks.

3. CHARACTERISTICS OF THE AVALANCHE PATHS FROM THE PARÂNG MOUNTAINS

A specific morphological feature of the avalanche paths from the Parâng Mountains is their development in a narrow valley sector which limits the lateral expansion of snow avalanches. The lateral slopes of the path become steeper the further away they are from the ridge. Neither in the accumulation zone nor in the rest of the path has any visible cone been identified as formed by the accumulation of sediments transported by snow avalanches (Pop et al., 2016).

The avalanche path from the Zăvoaie Valley is located in the north-western extremity of the Parâng ridge, north-east from the Parângul Mic Peak (2074 m), in the Zăvoaie Valley, a left tributary of the Mija Valley. The path developed on an incipient glacial valley (Fig. 3). The maximum altitude in the path is of approximately 2070 m, near the Parângul Mic Peak. The minimum altitude is of approximately 1100 m and is located at the confluence of the Zăvoaie and Mija valleys. The relative length of the path is 2.2 km, and the surface is 0.56 km^2.

The second avalanche path is also located in the north-western extremity of the Parâng Mountains, on the south-western slope of the Parângul Mic Peak, in the Scărița Valley, a tributary of the Izvorul Valley which flows into the Jiu, in the gorge sector (Fig. 3). The maximum altitude from this avalanche path is 2070 m, close to the Parângul Mic Peak. The minimum altitude is of approximately 1570 m. The length of the path is of 1 km, and the surface is 0.2 km^2.

In the vicinity of this avalanche path there is the Parâng ski area, including 11.5 km of ski slopes and 8 chairlifts. An expansion project for this ski resort is currently being implemented by the local council of Petroșani. This project includes, among others, 11 additional ski slopes and the lengthening of an existing slope with a total length of 12.66 km, 2 additional chairlifts which would reach the Parângul Mic Peak (2074 m), as well as a gondola lift which would leave from Petroșani and would reach the ski resort in the Slima area.

The third avalanche path we analyse in this study is located in the central part of the Parâng Mountains, still on the southern side of the main ridge, in the south-west of the Păpușa Peak (2135 m). This path developed between two branches of the main ridge of the Parâng Mountains, on a lateral slope of a former glacial valley. This valley is part of the upper catchment area of the Romanul River (Fig. 3), a tributary on the right of the Gilort. The

maximum altitude from this avalanche path is of approximately 2100 m. The minimum altitude is 1350 m, while its length is 1.6 km and its surface is 0.5 km^2.

The Transalpina road, which is currently still under construction, crosses the starting zone of the analysed avalanche path. However, no measures of protection against snow avalanches have been taken yet.

The fourth avalanche path is located as well in the central part of the Parâng Mountains, on the southern slope, in the south-west of the Păpușa Peak. The path covers an incipient glacial cirque and the upper sector of an incipient glacial valley. This is part of the upper catchment of the Mușet Valley, which is an indirect tributary of the Gilort. The maximum altitude in this path is approximately 2100 m. The minimum altitude is 1650 m. The length is approximately 1.3 km, and the surface is 0.6 km^2 (Fig. 3).

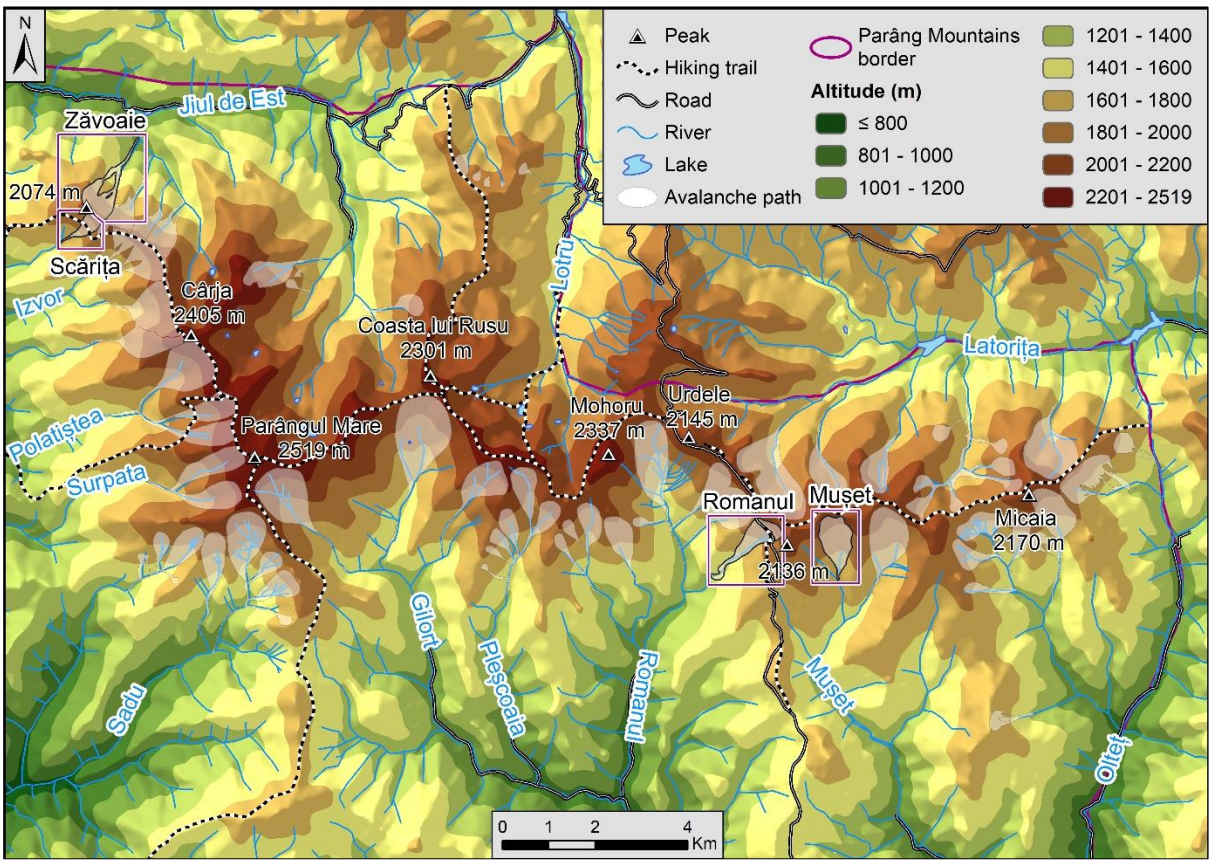

Fig. 3 The location of the analysed avalanche paths

4. CONCEPTS AND METHODOLOGY

The term dendrochronolgy derives from the Greek terms *dendron* (meaning tree), *chronos* (meaning time) and *logos* (meaning science). Dendrochronology is the science that studies tree rings in order to give answers to questions related to natural history (Wenk, 1999).

Dendrogeomorphology is based on the process-event-response principle founded by J. F. Schroder Jr (1978). This is a principle that can be applied to all geomorphological processes that can affect trees causing an event that disturbs the natural growth of trees in an affected area. Trees respond to the geomorphological process by diminishing as much as possible the growth disturbance by trying to recover as soon as possible the natural growth. These growth anomalies occur in the tree ring that is forming after the occurrence of the geomorphological process and sometimes also in the following rings (Stoffel and Bollschweiler, 2009).

4.1. Growth anomalies used to reconstruct snow avalanches

Compression wood (Fig. 4) grows only in coniferous trees. Mass slides lead to the formation of debris deposits at stem base, deposits that by pressing against the tree lead to its tilting (Stoffel and Bollschweiler, 2009).

The structure of cell walls in compression wood cells is different from the structure of regular wood cell walls and the difference lies in the presence of cellulose microfibers in the cell layers. During growth, cells in compression wood extend longitudinally in order to push the tree to its upwards original position (Du and Yamamoto, 2007).

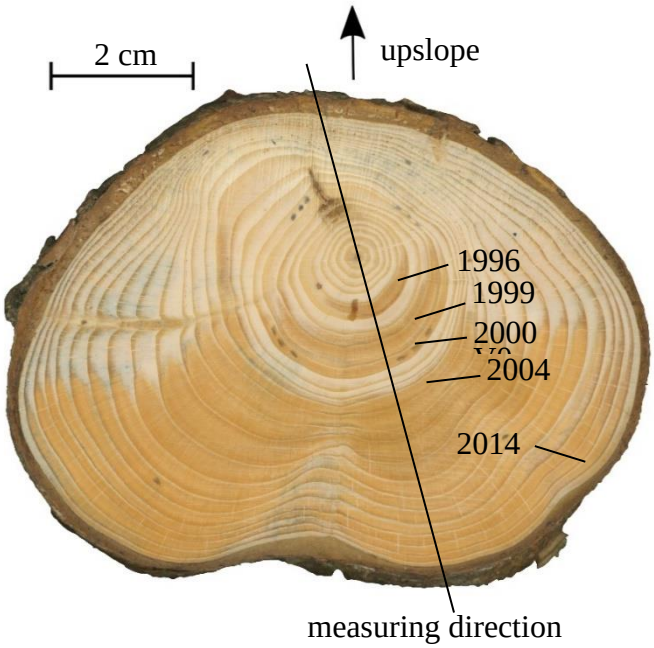

Fig. 4 Disk showing 3 areas of compression wood (1996, 1999-2000, 2004-2014)

Traumatic resin ducts (Fig. 5) are specific to coniferous trees. They appear as a result of the mechanical impact that leads to the partial destruction of cambium and thus a lesion is formed (Bollschweiler et al., 2008, Pop et al., 2012).

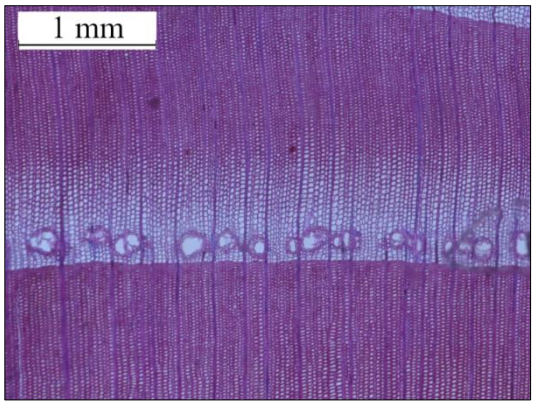

Fig. 5 Traumatic resin ducts at the beginning of an annual tree ring.

Traumatic resin ducts are distributed in tangential rows along the lesion in order to transport resin to the lesion with the purpose of closing it. This defense mechanism appears in 18 days after the impact (Nagy et al., 2000).

Growth is considered to be reduced (Fig. 6) once the width of annual tree rings is suddenly reduced by minimum 40% compared to neighboring rings. Depending on the intensity of the impact one or more rings can be reduced or one or more tree rings can be missing.

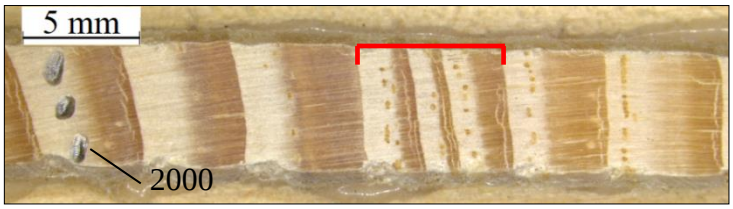

Fig. 6 Fragment of a core depicting reduced growth

Growth is considered to be released (Fig. 7) once the width of annual tree rings is suddenly increased with minimum 30% compared to the neighboring rings. The growth difference between two neighboring rings can be up to 200%. Growth release occurs mainly after events that led to the destruction of trees around the one under study. Consequently, without the competition of neighboring trees, the tree in question benefits from more light, water and/or nutrients thus resulting an increased growth visible in wider tree rings.

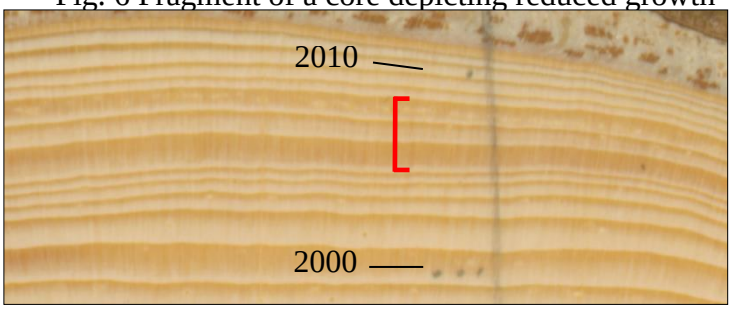

Fig. 7 Fragment of a scanned disk depicting growth release between 2005 and 2007

Scars (Fig. 8) result from the direct mechanical impact to the tree once the bark and significant areas of the cambium are damaged. Although at exterior level scars may be concealed with time, they are visible in cross sections or core samples collected around the

Fig. 8 Edge of an open scar

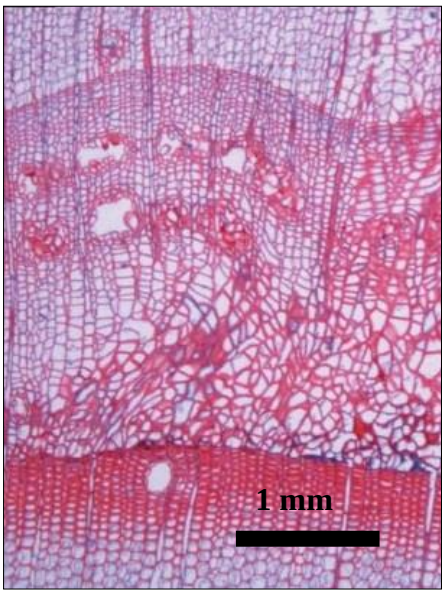

Fig. 9 Callus tissue (Stoffel and Bollschweiler, 2008)

tree was scarred can be identified by simply counting the annual rings formed in the proximity of the scar (Simea, 2012).

Callus tissue (Fig. 9) is the growth anomaly that appears always around a scar. In order to mitigate the risk of insect attacks, fungus or rotting, right after the impact causing a scar, the tree starts to produce layers of cells in chaotic shapes at the edges of the scar to be able to cover the scar as soon as possible. The cells in callus tissue are irregular in shape and distributed without a pattern. (Stoffel and Bollschweiler, 2009).

4.2. Methodology: Stages of the dendrogeomorphological reconstruction

The first step implies identifying one or several avalanche paths that descend low enough in the forest, beginning at the upper forest limit. The identification is done in the lab on cartographic documents like maps, topographic plans, aerial or satellite images, orthophotoplans etc. (Stoffel et al., 2013).

The second step implies collecting samples from trees affected by snow avalanches. Trees with visible marks of avalanche impact (scars, bended stems, pollarded trees etc.) are selected, as well as reference trees, meaning fully normally grown trees that grow aside along the avalanche path (Fritts, 1976). Tree sampling is done either by cutting disks (Fig. 4) or by boring for cores (Fig. 10).

Selecting the proper spot for core sampling is of great importance. Sampling of a tree with a bended stem in the lower section is to be done in the point of maximum curvature. A

scar can be dated by: (i) boring a core through the scar and a core on the opposite side, (ii) identifying the traumatic resin ducts in its proximity, (iii) by cutting a wedge at the edge of the scar, or (iv) by cutting a cross section. Sampling of a pollarded tree is to be done below the level of the first pollarding. Flag-shaped trees (that have branches only down-slope) and dried trees can also be sampled.

Fig. 10 Increment cores in a polycarbonate sheet

In order to analyse the samples in the lab, the following preparatory steps must be completed: drying, sandpapering and marking the tree rings every 10 years. The measurement of tree rings is performed on a microscope with mobile table (*LINTAB 5station* (RINNTECH, 2016)), connected to a computer that records the measurements in a specialized software (*TSAPWin Professional 0.22* (RINNTECH, 2016)) or a more recent version (Fig. 11).

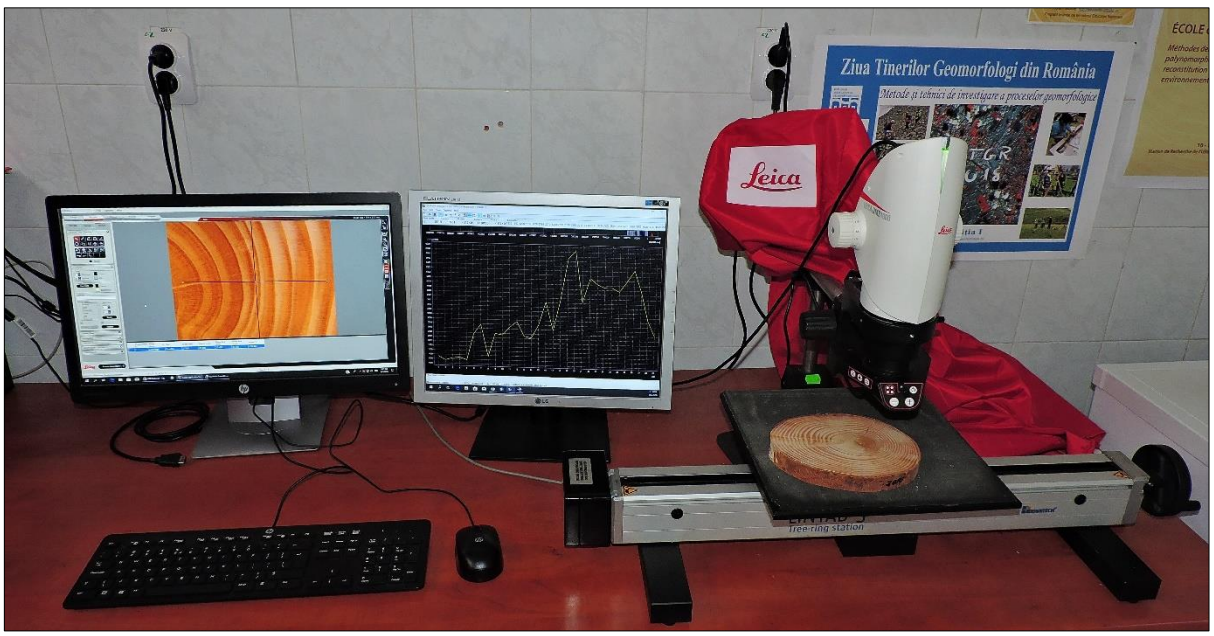

Fig. 11 LINTAB 5 station and the microscope Leica DMS 1000 connected to a computer

During or after the measurements, growth anomalies are being identified, classified according to intensity (A - high, B - medium, C-low) and centralized. The age of the sampled trees is also noted down. In order to centralize the data more easily, personalised functions have been written in the Visual Basic language of Microsoft Excel.

Growth anomalies that occurred in the first 10 years from the lifespan of trees are not being taken into consideration in dating snow avalanches (Luckman, 2010, Pop et al., 2016).

Therefore, the number of sampled trees (visible in the graphs in Fig. 14, Fig. 18, Fig. 22, Fig. 26) which was taken into analysis is reduced to include only trees older than 10 years.

Three semiquantitative indices are being calculated according to the number of growth anomalies for each type of anomaly. The Avalanche Activity Index (AAI), identified by J. F. Schroder (1978) is the first index to be calculated according to the formula below:

$$AAI = \left(\sum_{i=1}^{n} Rt \Big/ \sum_{i=1}^{n} At\right) \times 100$$

Where *Rt* is one tree that had at least one growth anomaly in year *t*, and *At* is one of the sampled trees of 10 years minimum age.

Table 1 Growth anomaly intensity classified according to (Stoffel and Corona, 2014)

Intensity	Growth anomalies
Intensity 5	Impact scars Strong traumatic resin ducts
Intensity 4	Kill date Moderate traumatic resin ducts Callus tissue Strong decrease in vessel lumen area and/or vessel number Strong reaction wood Strong growth reduction
Intensity 3	Moderate reaction wood Moderate growth reduction
Intensity 2	Strong growth release Weak reaction wood
Intensity 1	Weak traumatic resin ducts Moderate growth release

The second semiquantitative calculated index is the weighted avalanche activity index (*Wit*), defined by Kogelnig-Mayer et al. (2011). It classifies and weights trees that have growth anomalies by the most severe registered growth anomaly, according to the recommendations of Stoffel and Corona (2014) (Table 1). The index was calculated according to the following formula (Pop et al., 2018):

$$Wit = \left(\left(\sum_{i=1}^{n} T_5 \times 5\right) + \left(\sum_{i=1}^{n} T_4 \times 4\right) + \left(\sum_{i=1}^{n} T_3 \times 3\right) + \left(\sum_{i=1}^{n} T_2 \times 2\right) + \left(\sum_{i=1}^{n} T_1 \times 1\right)\right) \times \frac{\sum_{i=1}^{n} Rt}{\sum_{i=1}^{n} At}$$

where T_5 is a tree whose growth anomalies in year *t* were classified as anomalies of intensity 5, T_4 is a tree whose growth anomalies in year *t* were classified as anomalies of

intensity 4, T_3 is a tree having intensity 3 anomalies in year *t*, T_2 is a tree having intensity 2 anomalies in year *t*, T_1 is a tree having intensity 1 anomalies in year *t*, *Rt* is a tree having at least one growth anomaly in year *t*, while *At* is a sampled tree that was alive in year *t*.

The third index is the Regional Avalanche Activity Index (RAAI). It is used to conclude on a regional scale over reconstructions of snow avalanches estimated for multiple avalanche paths when the analysis of avalanche activity on a larger area is performed. The index is calculated for each year when snow avalanches were registered, using the following formula:

$$RAAIt = \left(\sum_{i=1}^{n} AAIt \;\Big/\; \sum_{i=1}^{n} Ct\right) \times 100$$

where AAIt is the index of snow avalanche activity calculated for an avalanche path in the study area in year *t*, while *Ct* is an avalanche path in the study area where at least 10 trees out of the sampled ones were 10 years old in year *t*.

In order to select the years when snow avalanches occurred, the following criteria were considered: (i) the value of index AAI to be of at least 10%, (ii) the existence of at least one growth anomaly of intensity 4 or 5 according to the classification established by Stoffel and Corona (2014) (Table 1), (iii) the presence of growth anomalies in minimum 3 sampled trees, (iv) and minimum 10 sampled trees to have been alive then.

The Avalanche return period (*Rp*) is the time span while avalanches slide a certain distance or pass over a certain location (McClung and Schaerer, 2006). It is calculated using the following formula:

$$Rp = \frac{\Delta t}{Na}$$

where Δt is the duration of an interval in years, while *Na* is the number of snow avalanches registered during the same period of time (Boucher et al., 2003).

Previously, the avalanche return period was calculated using the methodology of Reardon et al. (2008). It implies calculating the return period for each tree separately by dividing the tree age to the number of registered avalanches. Subsequently, these values are interpolated using the *Ordinary Kriging* method. This method was used to calculate the return period of snow avalanches in the avalanche paths Zăvoaie, Scărița and Romanul (Meseșan et al., 2018a).

A new methodology was proposed in order to eliminate interpolation and the calculation of avalanche return period for each tree from the methodology of calculating the return periods of avalanches (Meseșan et al., 2018a). Using the Python 2.7.5 programming language, a script was developed that determines automatically the number of avalanches that

affected each pixel of the avalanche path. It was successfully loaded in QGIS version 2.18.0 (QGIS Development Team, 2016), that corresponds to SAGA GIS version 2.1.2. The script requires the following data: a digital elevation model, limits of avalanche path and the positioning of sampled trees. The execution steps of this script are detailed in figure 12. By dividing the reconstructed chronology of snow avalanches to the result of the script using *QGIS Raster Calculator*, the return period for each pixel of the avalanche path is being determined.

4.3. Reconstruction of snow avalanche extent using remote sensing

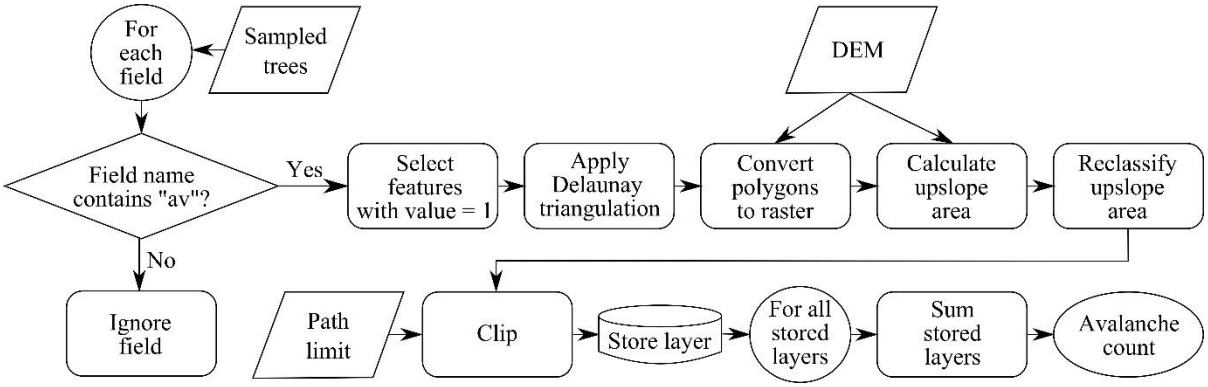

Fig. 12 Execution steps of the script that calculates the number of avalanches

The methodology used to reconstruct the extent of snow avalanches with remote sensing is detailed in the paper written by Meseșan et al. (2018b). 20 Landsat images (5TM and 7 ETM+) of Surface Reflectance processing level (Masek et al., 2006) were downloaded to cover the study area. In order to identify the areas affected by the snow avalanche that occurred in the winter of 1985-1986, 5 Landsat 5TM images were selected and the following spectral indices were calculated for them: normalized burn ratio (NBR) (López García and Caselles, 1991), normalized difference moisture index (NDMI) (Goodwin et al., 2008), moisture stress index (MSI) (Rock et al., 1985) and disturbance index (DI) (Healey et al., 2005). The calculation formulas of the indices are detailed below. The DI index uses as input the 3 vectors that result from the transformation Tasseled cap (Kauth and Thomas, 1976).

$$NBR = \frac{Band\ 4 - Band\ 7}{Band\ 4 + Band\ 7} \qquad NDMI = \frac{Band\ 4 - Band\ 5}{Band\ 4 + Band\ 5}$$

$$MSI = \frac{Band\ 5}{Band\ 4}$$

$$DI = Luminosity - (Green\ ratio + Humidity)$$

The indices calculation was followed by the identification of polygons (the equivalent of pixels) where the NBR and NDMI indices are lower than the threshold value of 0.08 while the MSI index exceeds that value. There is no pattern in the variation of DI index and no

threshold could be set up. Consequently, for DI only the value increase was taken into consideration.

The spectral trajectory of pixels that had significant variation due to the analysed avalanche was captured in graphs. In the case of this study they are a viable alternative for the LandTrendr model (Kennedy et al., 2010).

IBM SPSS Statistics v. 22 (IBM, 2011) was used to evaluate the correlation between the location of the areas previously identified as being affected by the snow avalanche in the winter of 1985-1986 and the location of the sampled trees for which logistic regression was used (Dayton, 1992). The following tests were performed: Hosmer–Lemeshow (Hosmer Jr et al., 2013), square Cox and Snell R (Cox and Snell, 1989) and square Nagelkerke R (Nagelkerke, 1991).

4.4. Reconstruction of meteorological conditions associated with the triggering of snow avalanches

The meteorological conditions which have determined the triggering of snow avalanches in the past are relatively the same in the present. Knowing the connection between the variation of the meteorological parameters and the past activity of snow avalanches can facilitate a better anticipation of these phenomena (Birkeland et al., 2001). The connection between meteorology and the triggering of snow avalanches is a complex one due to the non-linearity of the processes which operate in the developing snow layer (Keylock, 2003).

In the present study, the following daily meteorological data have been processed: average temperature, maximum temperature, minimum temperature, amount of precipitation, thickness of snow layer, maximum wind speed, average wind speed, all recorded at the Parâng meteorological station, between 1961-2013, in the months of November-March. Based on these data, 34 statistical parameters were computed, for each month from the mentioned interval, and were eventually used as independent variables in a stepwise multiple regression, performed with the IBM software SPSS Statistics v. 22. The Regional Avalanche Activity Index (RAAI) for the time interval of 1961-2015 was used as a dependent variable.

5. RESULTS

5.1. Results of the dendrogeomorphological reconstruction

In order to identify the normal growth of the trees from the study area, 48 trees which were unaffected by avalanches or other geomorphological processes were analysed. The reference curve with values expressed in millimeters and the standardised growth curve are illustrated in Fig. 13.

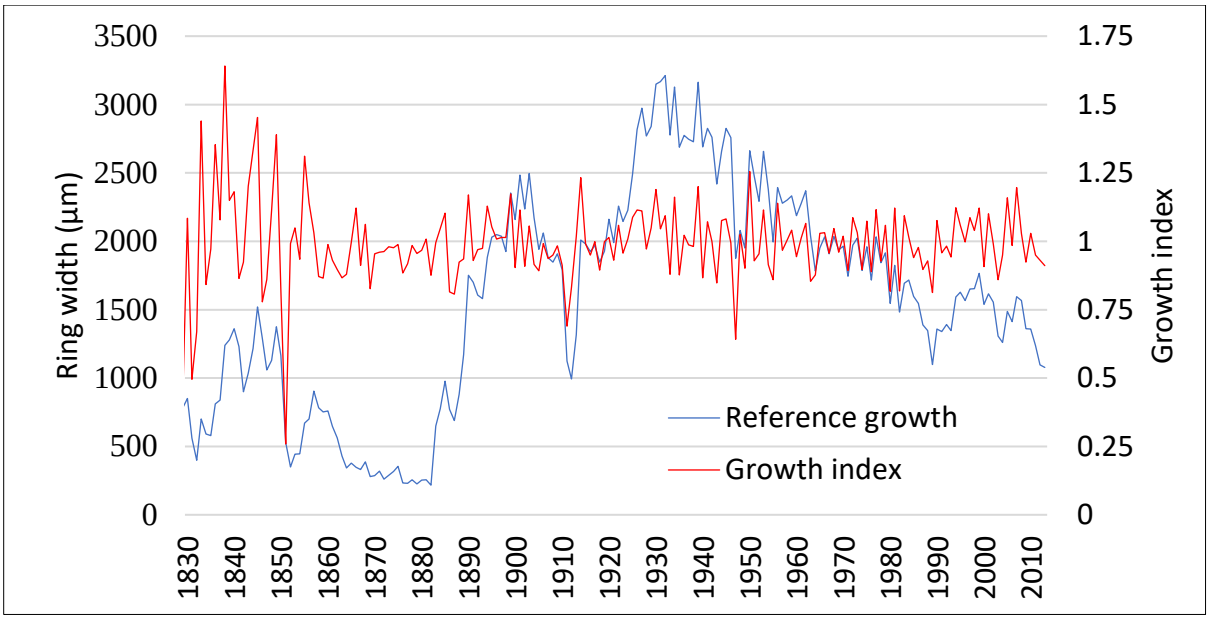

Fig. 13 Reference curve and growth indices for reference trees in the study area

5.1.1. The reconstruction of snow avalanche activity in the Zăvoaie path

In this avalanche path, 57 spruce trees were sampled which presented visible marks left by the impact with snow avalanches. 113 increment cores and 3 disks resulted. In addition to these, 3 wedges from 3 sycamore trees were sampled, their stems presenting scars.

After the analysis of all these samples, 227 growth anomalies were identified, which have led to the certain reconstruction of 12 years with snow avalanches: 2008, 2005, 2001, 1999, 1997, 1986, 1983, 1966, 1956, 1942, 1937 and 1915. Half of the reconstructed avalanches have caused a scar in the sampled trees. The values of the Avalanche Activity Index (AAI), calculated based on the samples taken from this avalanche path, are presented in Fig. 14, and the values of the weighted index of snow avalanche activity (Wit) are presented in Fig. 15.

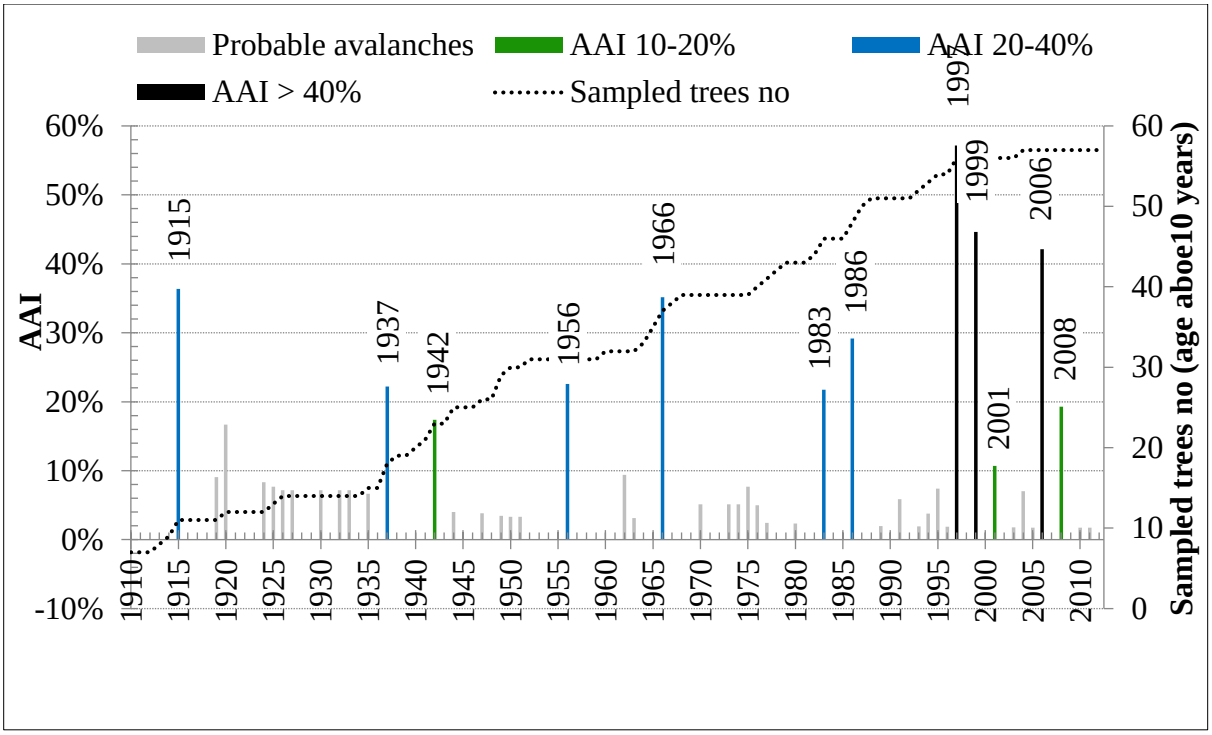

Fig. 14 Histograms representing the reconstructed avalanches from the Zăvoaie path, classified according to the AAI value

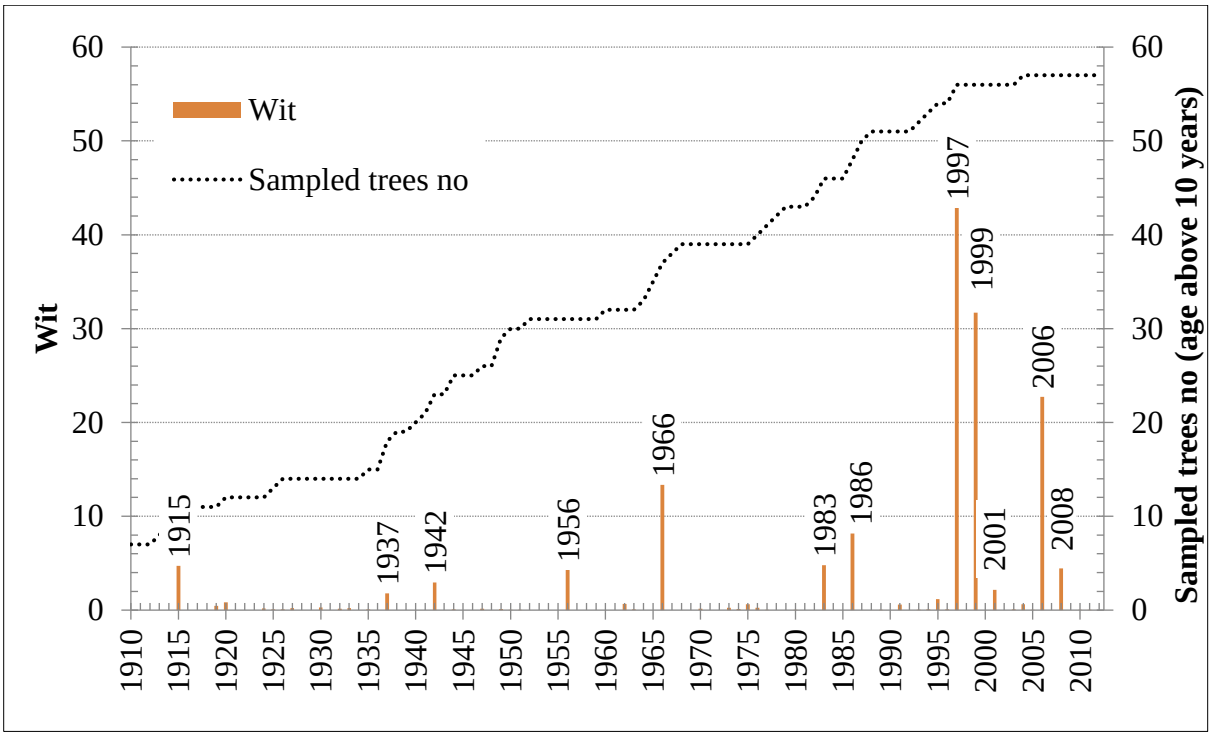

Fig. 15 Values of the weighted index of snow avalanche activity for the Zăvoaie path

The return period of avalanches, calculated for each tree separately, according to the existent method, is presented in Fig. 16. The return period of avalanches, calculated with the proposed method, is presented in Fig. 17.

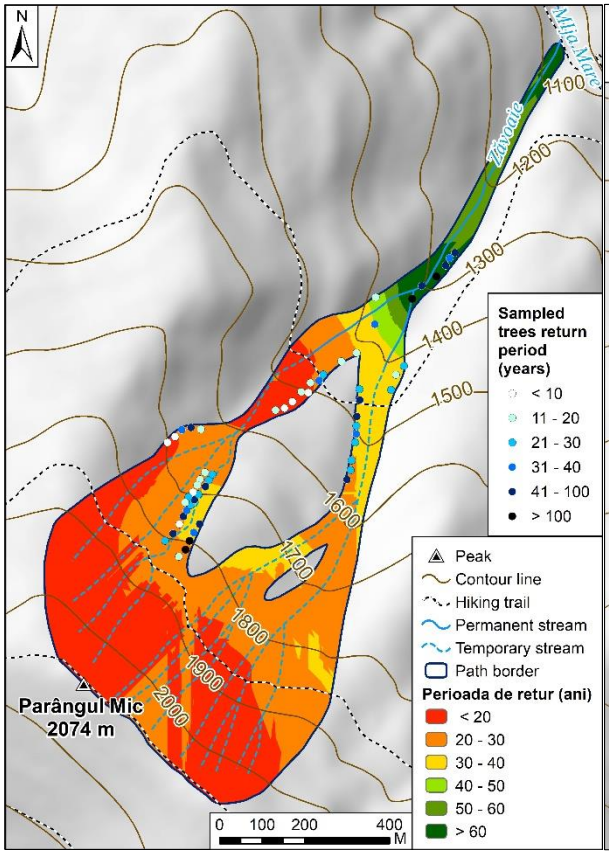

Fig. 17 The Zăvoaie avalanche path – return period calculated with the existent method

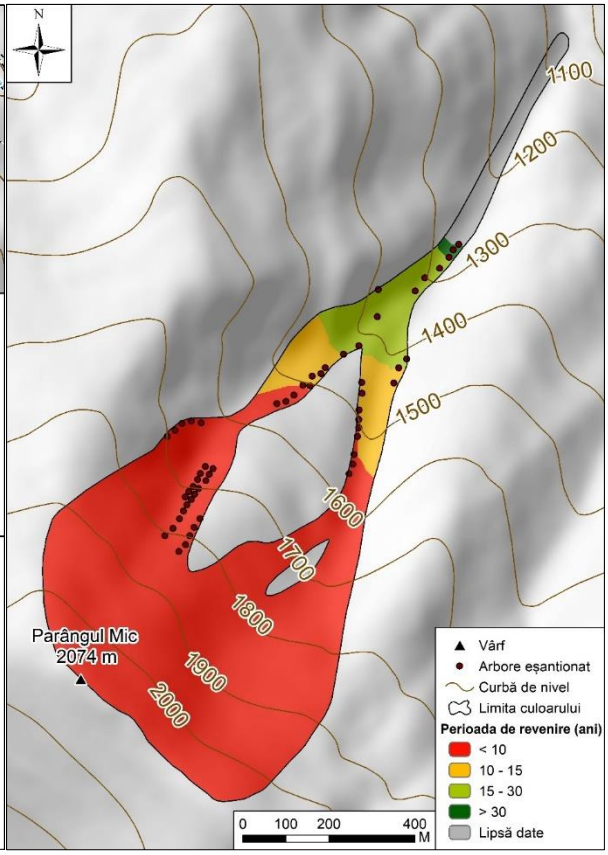

Fig. 16 The Zăvoaie avalanche path – return period calculated with the proposed method

5.1.2. The reconstruction of snow avalanche activity in the Scărița path

In this avalanche path 116 spruce trees were sampled which presented visible marks from the impact of snow avalanches. 222 increment cores and 14 disks were sampled. In addition to these, a wedge was sampled from an older spruce tree with a thick tree stem which presented a scar.

After analysing the samples from this avalanche path, 676 growth anomalies were identified which led to the certain reconstruction of 21 years in which snow avalanches occurred: 2012, 2010, 2008, 2005, 2003, 1999, 1997, 1995, 1990, 1987, 1986, 1982, 1980, 1976, 1970, 1966, 1959, 1950, 1944, 1942, 1938. The values of the Avalanche Activity Index (AAI), which are calculated based on the samples taken from this avalanche path, are presented in Fig. 18. The values of the weighted index for avalanche activity (Wit) in this avalanche path are presented in Fig. 19.

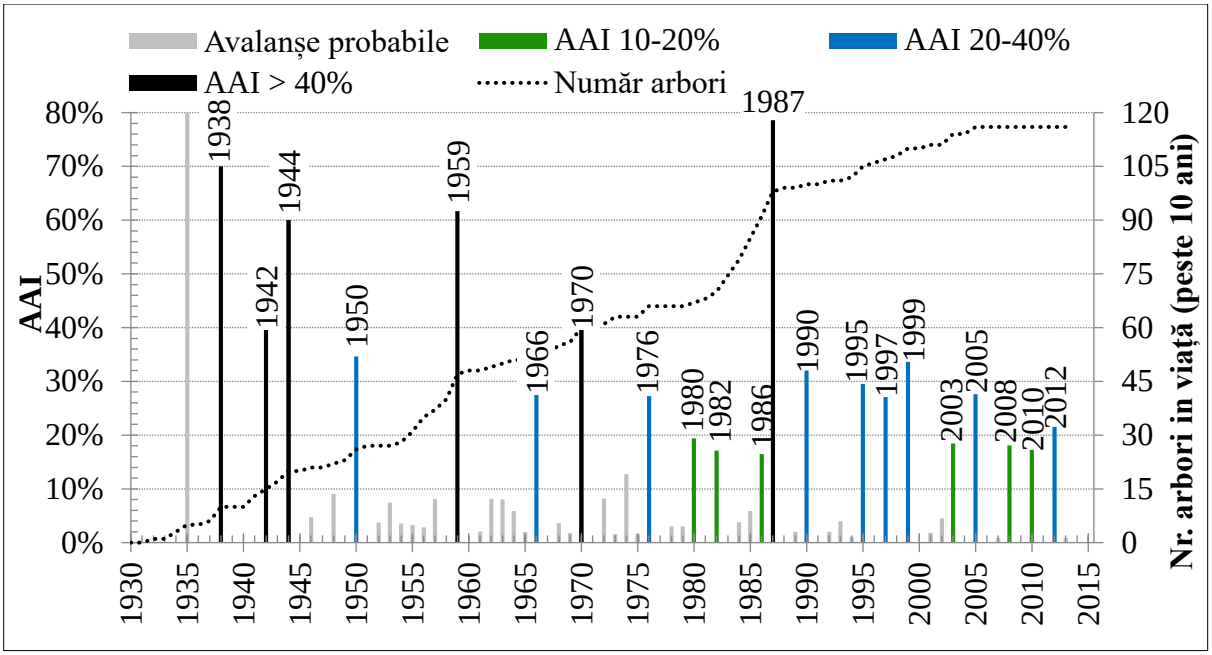

Fig. 18 Histograms representing the reconstructed avalanches from the Scărița path, classified according to the AAI values

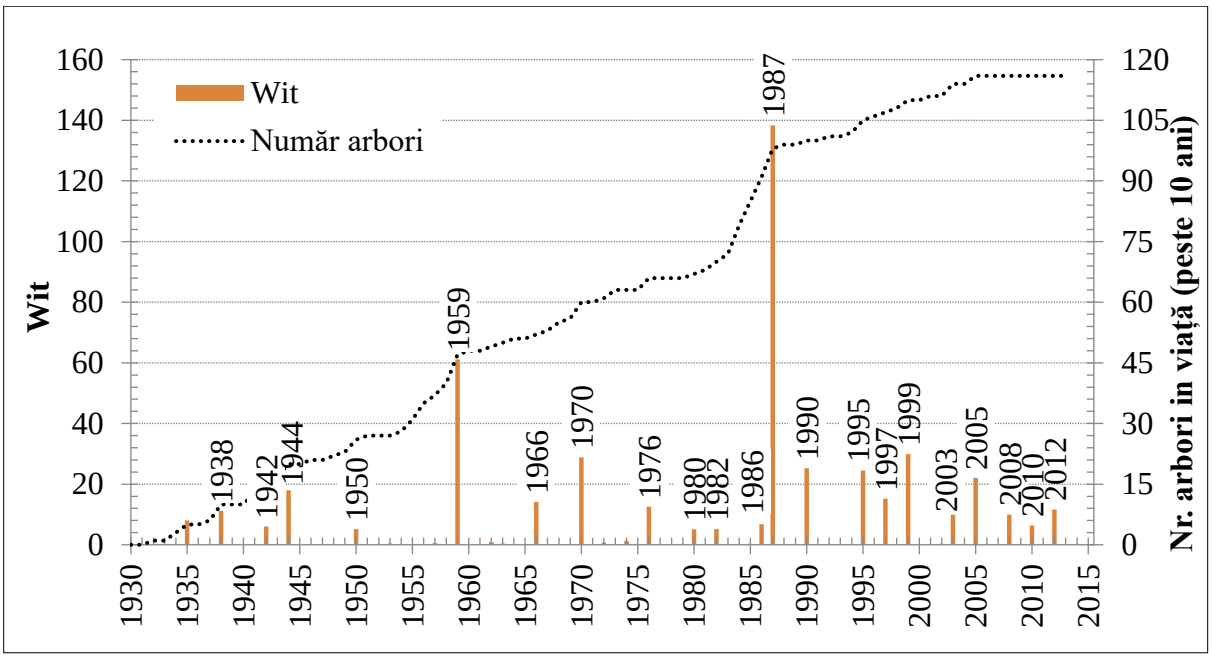

Fig. 19 Values of the weighted index of avalanche activity for the Scărița path

The return period of snow avalanches was calculated for each tree separately according to the existent method and is presented in Fig. 20. The return period of avalanches calculated with the proposed method is presented in Fig. 21.

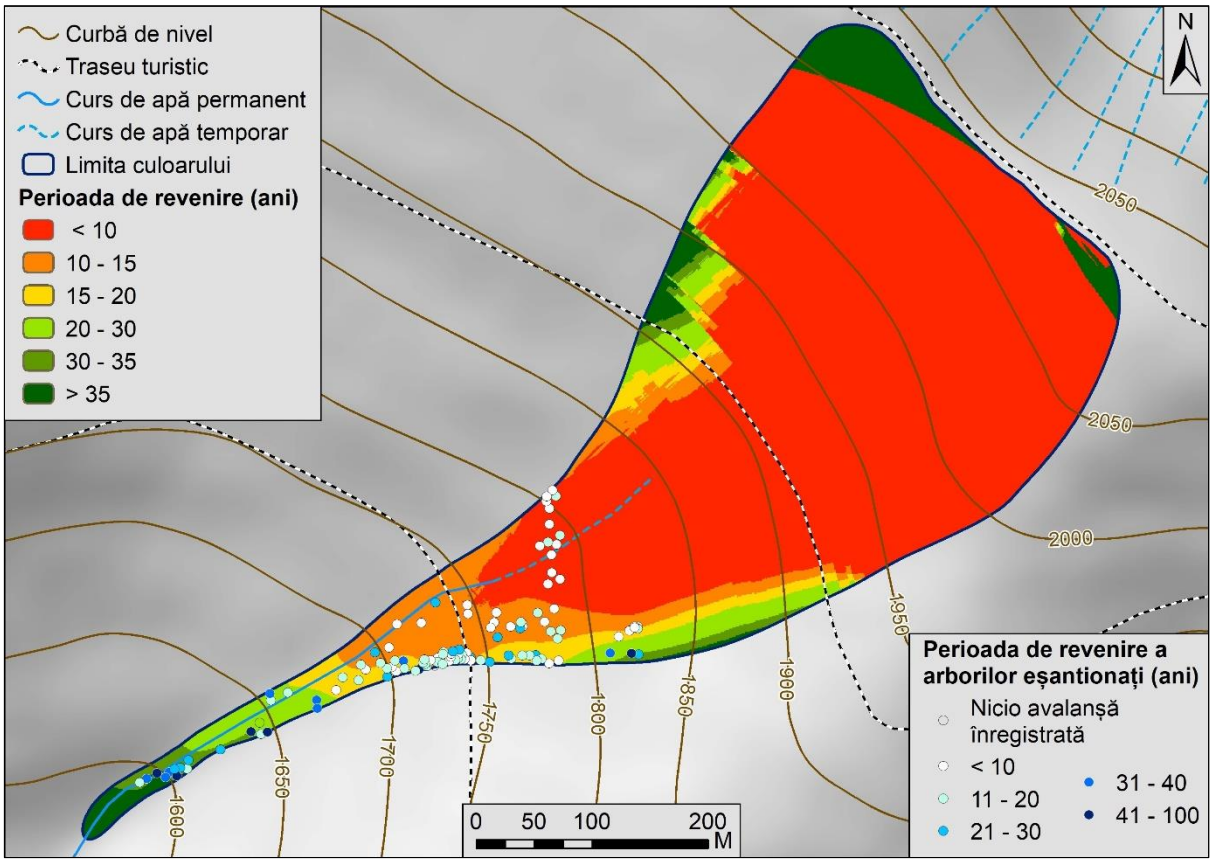

Fig. 20 Scărița avalanche path – the return period calculated with the existent method

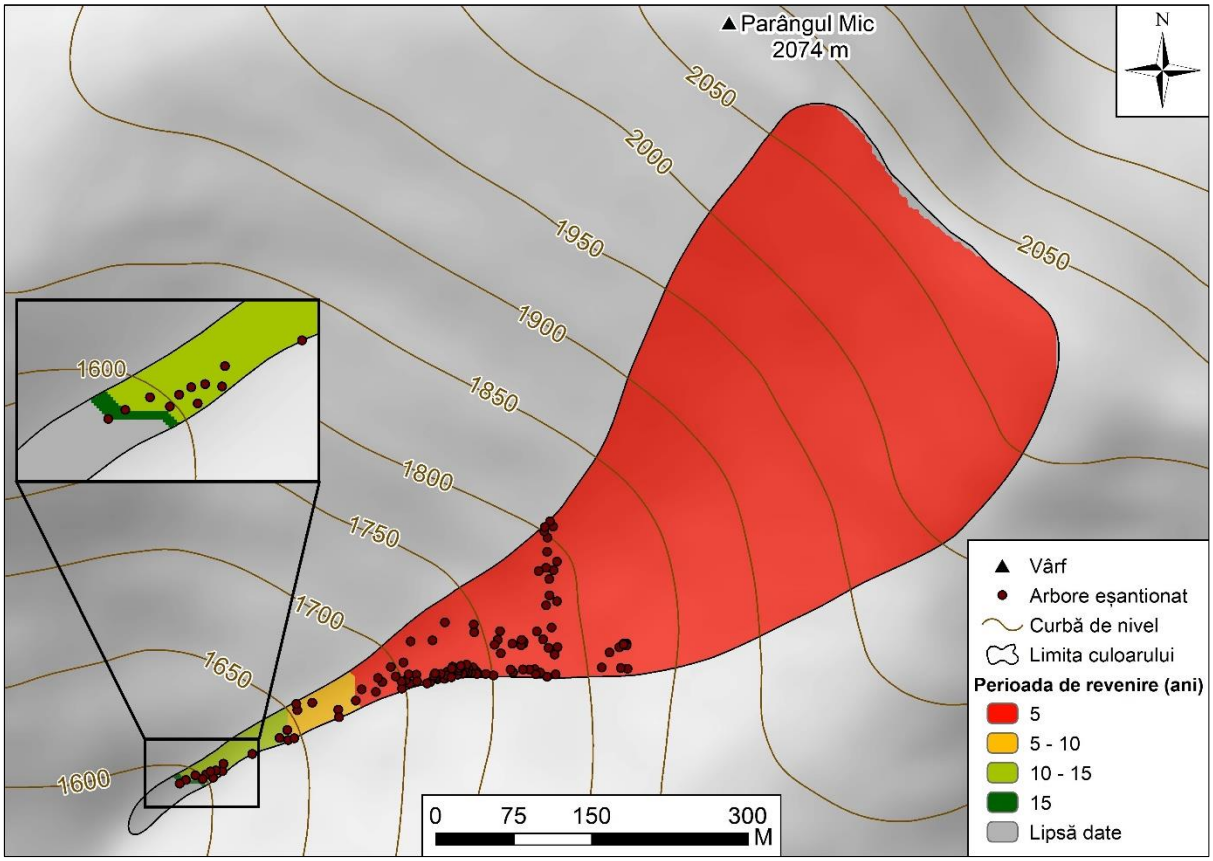

Fig. 21 Scărița avalanche path – the return period calculated with the proposed method

5.1.3. The reconstruction of snow avalanche activity in the Romanul path

In this avalanche path 58 spruce trees were sampled from which the majority presented visible marks of the impact with snow avalanches. 95 increment cores and 22 disks were sampled. In addition to these, another disk was sampled from a rowan (*Sorbus aucuparia* L.) which presented a scar caused by the impact of a snow avalanche.

After analysing the samples taken from this avalanche path, 212 growth anomalies were identified which enabled the certain reconstruction of 11 years in which snow avalanches occurred: 2013, 2012, 2008, 2006, 2005, 2003, 2000, 1998, 1996, 1991, 1988. In 1895, out of 9 trees which were over 10 years old, 8 trees presented clear marks of the mechanic impact of a snow avalanche, including a scar. All these trees were located in the upper part of the path, close to its western limit. In this particular year, the occurrence of a snow avalanche cannot be certainly attested as there were only 9 trees over 10 years old which were sampled. The values of the Avalanche Activity Index (AAI), calculated using the samples taken from this path, are presented in Fig. 22. The values of the weighted index of avalanche activity (Wit) are presented in Fig. 23.

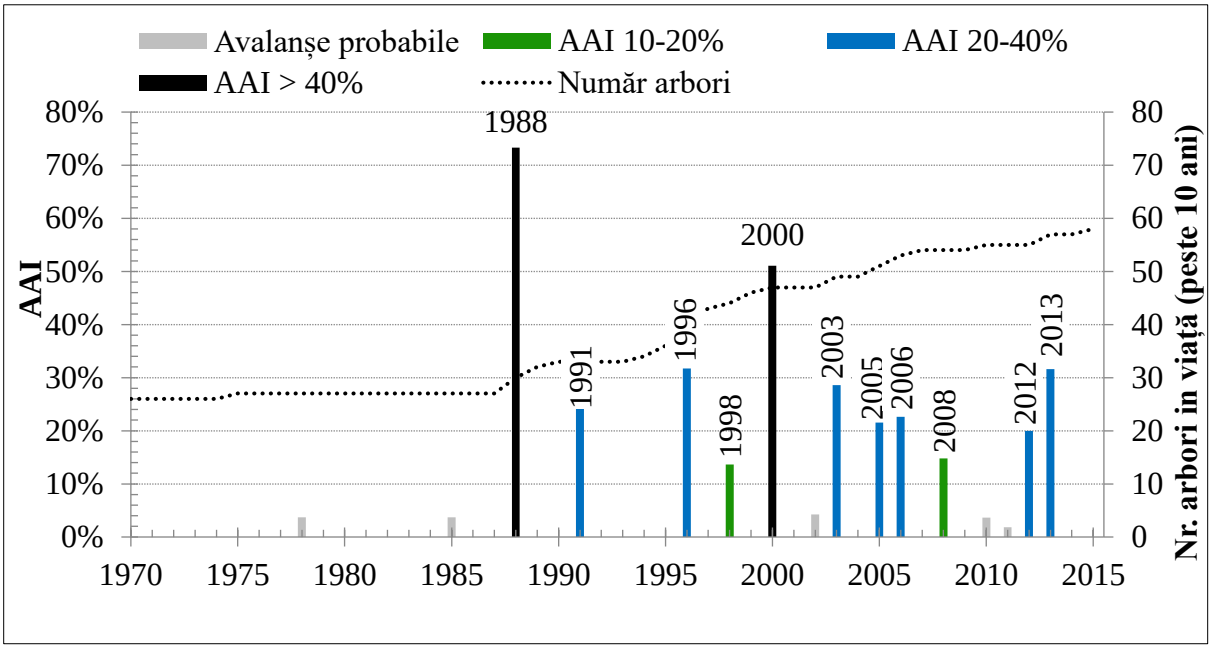

Fig. 22 Histograms representing the reconstructed avalanches from the Romanul path, classified according to the AAI values

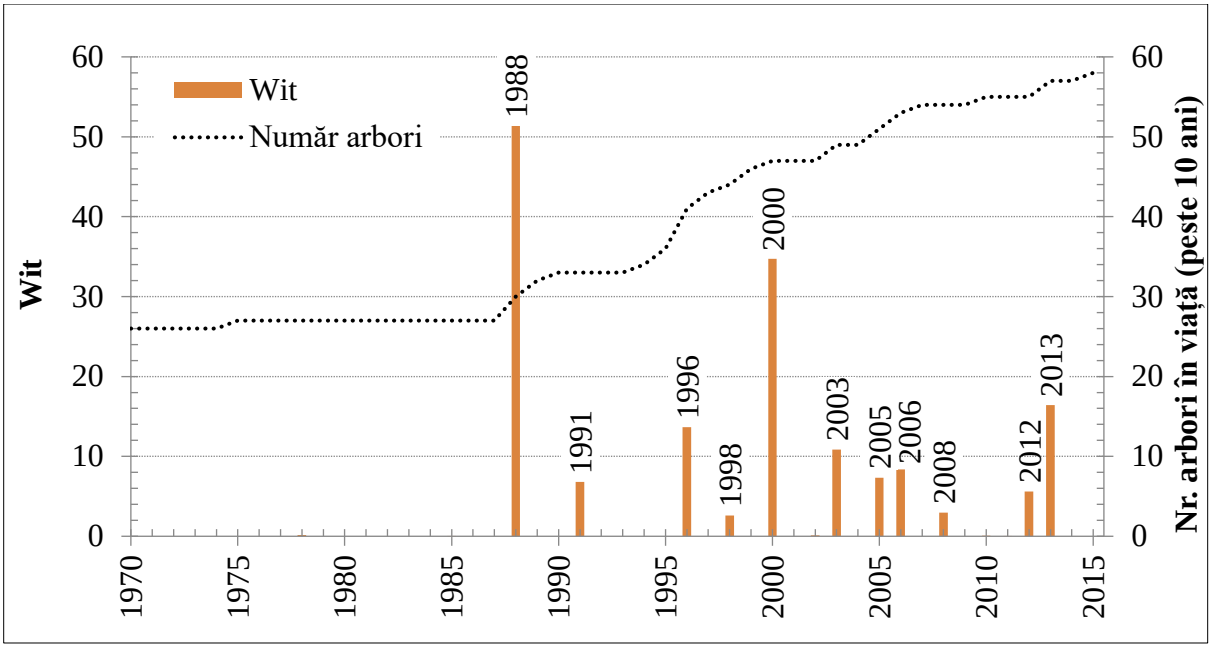

Fig. 23 Values of the weighted index of avalanche activity for the Romanul path

The return period for avalanches, calculated for each tree separately, according to the existent method, is presented in Fig. 24. The return period of avalanches calculated for this path with the help of the proposed method is presented in Fig. 25.

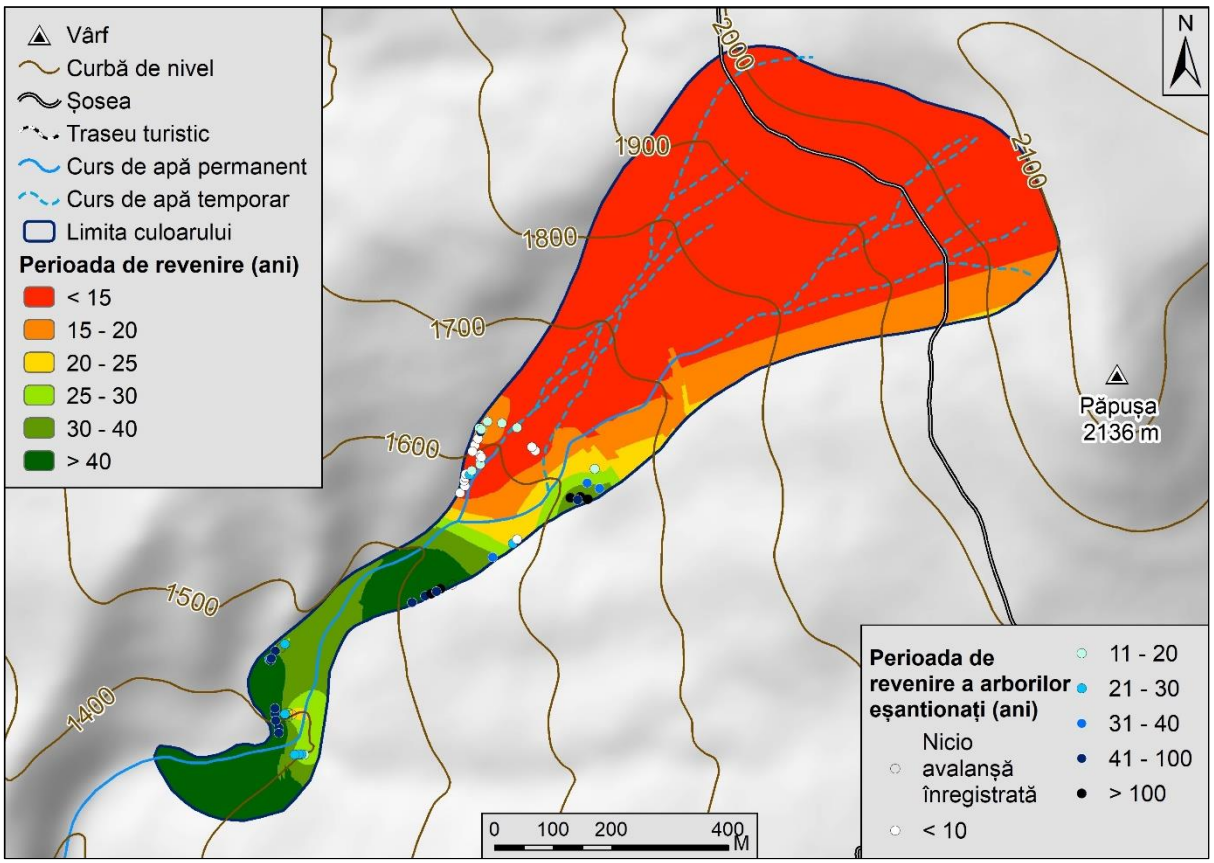

Fig. 24 Romanul avalanche path – the return period calculated with the existent method

Fig. 25 Romanul avalanche path– the recurrence interval calculated with the proposed method

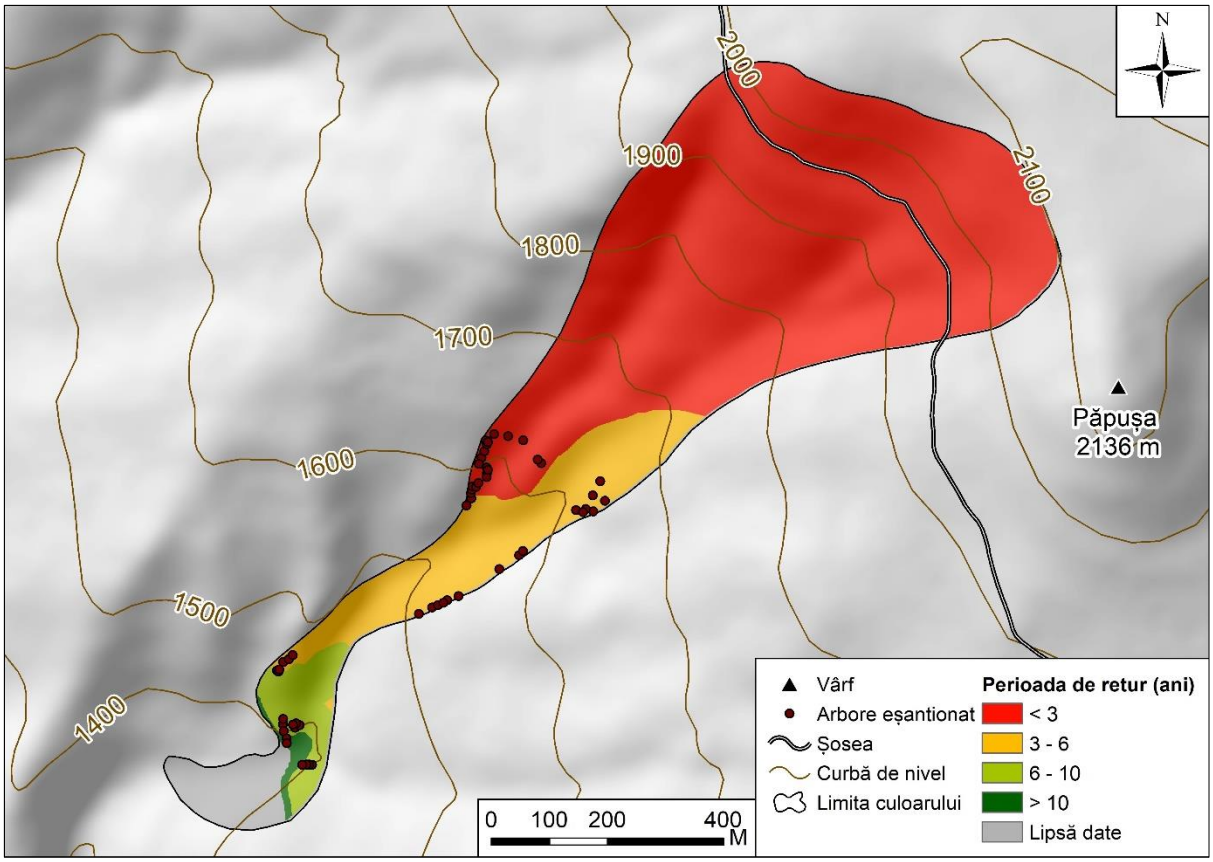

5.1.4. The reconstruction of snow avalanche activity in the Mușet path

In this avalanche path 52 spruce trees which presented visible marks of the impact of snow avalanches. 37 increment cores and 38 disks were sampled. Most of the sampled trees from this path were found in a grove of trees located above the upper limit of the forest.

After the analysis of the samples taken from this path, 146 growth anomalies were identified, which enabled the certain reconstruction of 10 years in which snow avalanches occurred: 2012, 2010, 2008, 2005, 2003, 1999, 1997, 1991, 1983, 1975. Among the reconstructed avalanches, with the exception of the one from 1983, all the other avalanches produced at least a scar in the sampled trees. The values of the Avalanche Activity Index (AAI), calculated based on the samples taken from this paths, are presented in Fig. 26, and the values of the weighted index for the avalanche activity (Wit) are presented in Fig. 27.

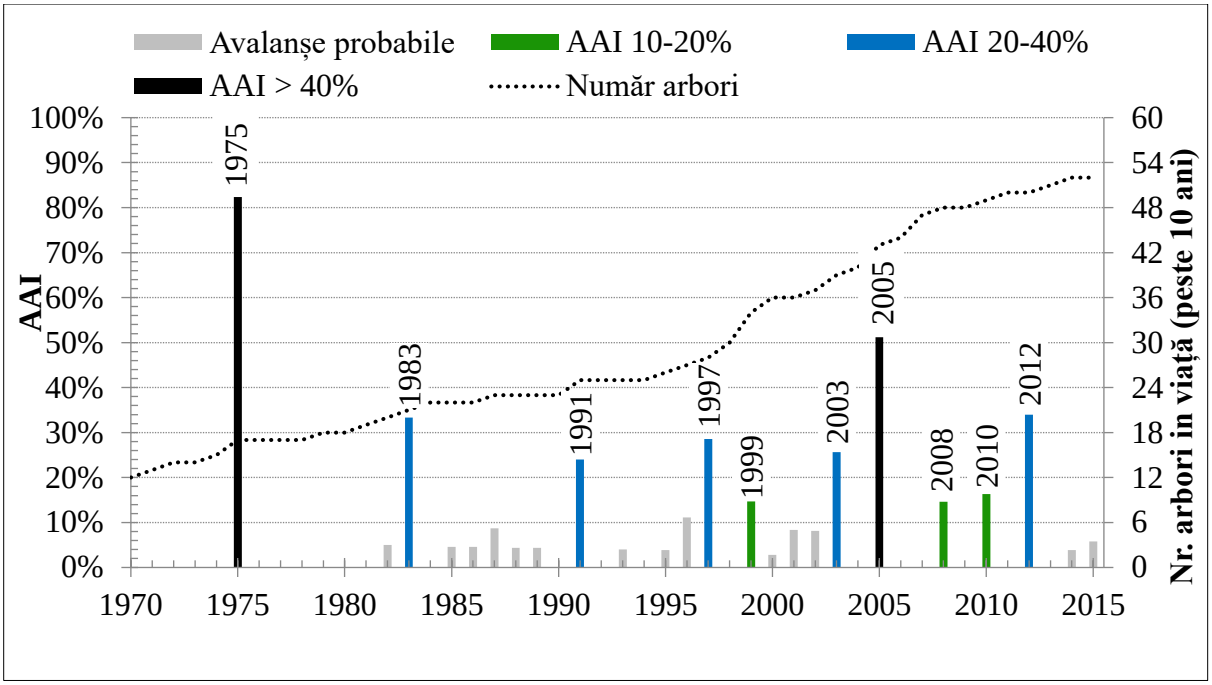

Fig. 26 Histograms representing the reconstructed avalanches from the Mușet path, classified according to the AAI values

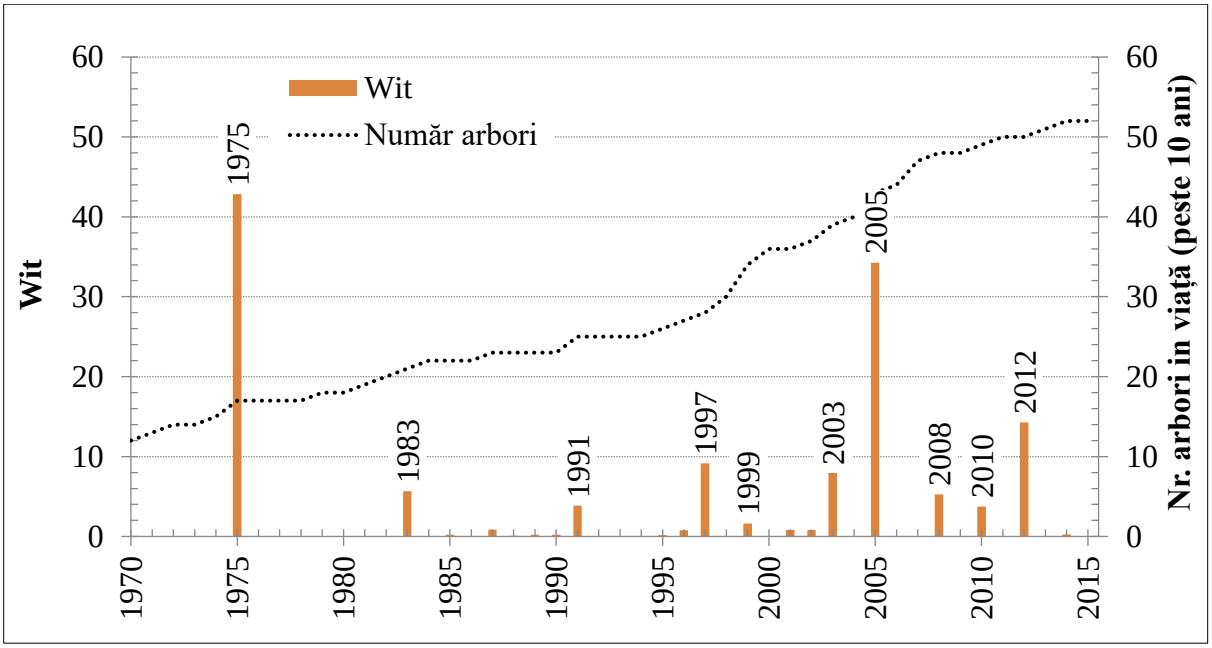

Fig. 27 The values of the weighted index of avalanche activity for the Mușet path

Taking into consideration the concentration of all the sampled trees on a small area from the avalanche path, the return period of snow avalanches was not calculated with the existent method so that the data would not be extrapolated from a very small area to the whole path. The return period, calculated with the proposed method, is presented in Fig. 28.

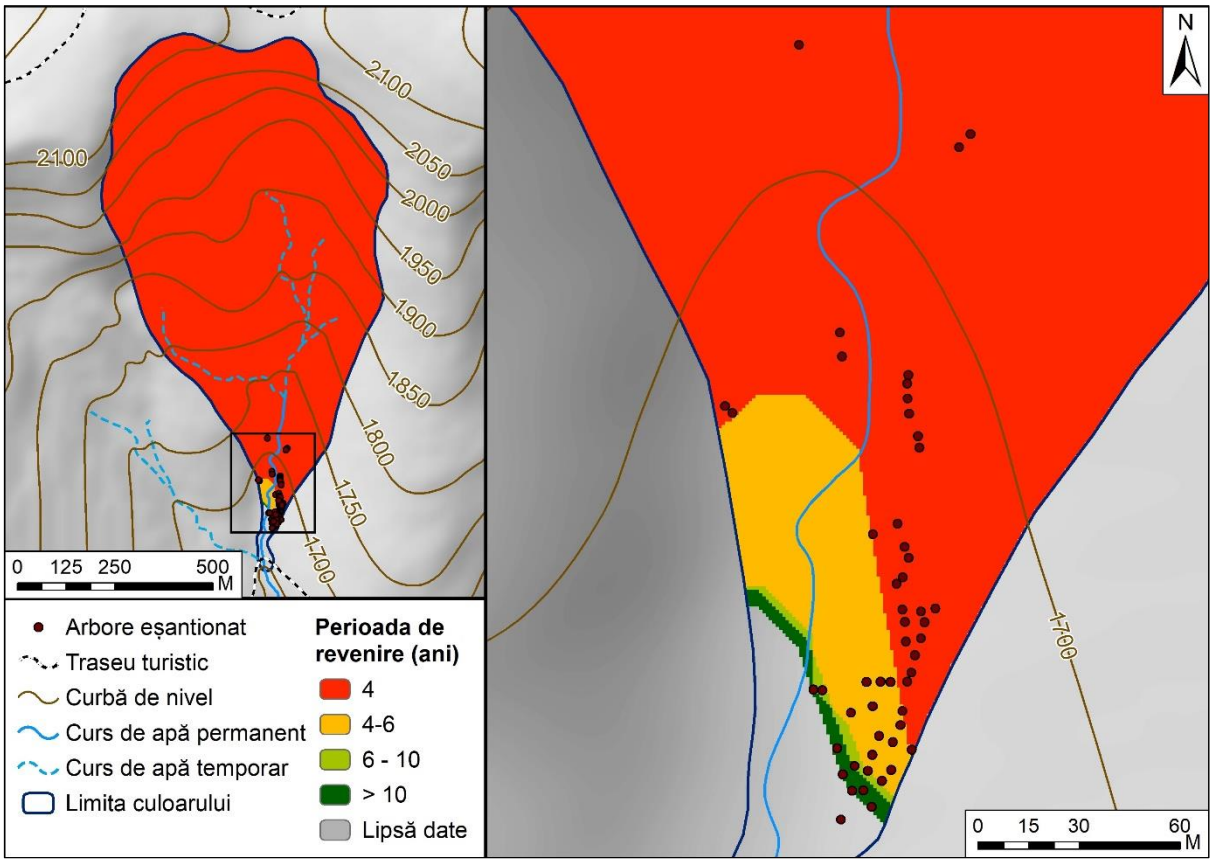

Fig. 28 Mușet avalanche path – return period calculated with the proposed method

5.1.5. The regional reconstruction of avalanche activity

The reconstructions of avalanche activity in the present study highlight two years in which snow avalanches occurred in all the four avalanche paths which were analysed (2005 and 2008). In three out of the four avalanche paths, avalanches were identified in the years 1997, 1999, 2003 and 2012 (Fig. 29).

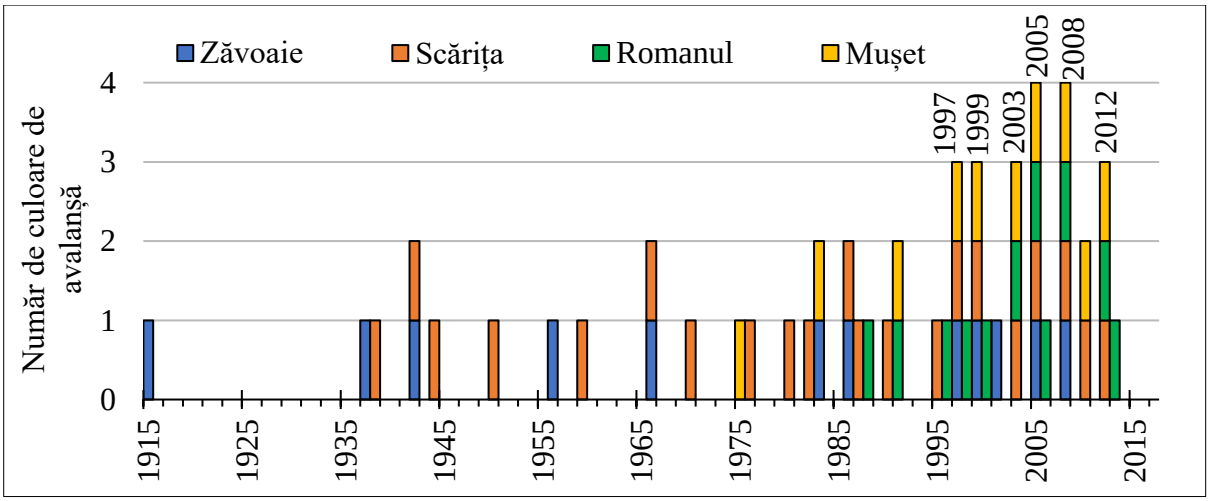

Fig. 29 The number and year of occurrence for the reconstructed avalanches from the analysed avalanche paths

The activity of snow avalanches at a regional level can also be captured through the Regional Avalanche Activity Index (RAAI). The values of this index, calculated for the four analysed paths, are presented in Fig. 30.

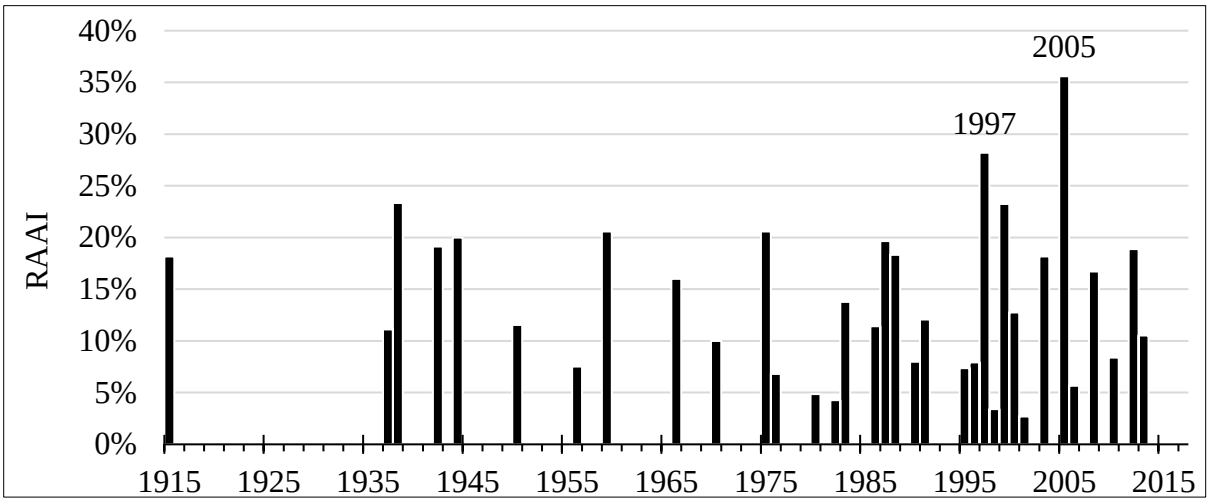

Fig. 30 The Regional Avalanche Activity Index calculated for the four paths analysed in the present study

5.1.6. The evaluation of the correlations between AAI, Wit, altitude and snow avalanche runout distance

The correlation between the minimum runout distance of the reconstructed snow avalanches and the Avalanche Activity Index, has low determination coefficients, below 0.3 for each avalanche path. These coefficients demonstrate the fact that the reconstructed magnitude of the snow avalanches is not influenced by their runout distance.

The correlation between the AAI and the altitude from the path where the snow avalanches stopped also has low values of the determination coefficients, except for the Zăvoaie path, where the R^2 values are higher than 0.3

The correlation between AAI and Wit has high values of the determination coefficient, 0.8-0.9 in all the analysed paths, with the exception of the Scărița path. As a consequence, both indices capture the same data variability in a proportion of 80-90%.

The minimum and maximum values of Wit which were recorded in the analysed paths (Zăvoaie 1.77 – 42.85, Scărița 5 – 138.28, Romanul 2.59 – 51.33, Mușet 1.61- 42.82) seem to be influenced by the number of sampled trees in the four avalanche paths. That is why we consider that a threshold value for the Wit index cannot be established in order to be applied to any snow avalanche path and to indicate that in a particular winter a snow avalanche certainly occurred.

5.2. The advantages and limitations of the proposed method for calculating the recurrence intervals

The interpolated values of the return period for avalanches, determined with the help of the existent method, are considerably higher than the values determined with the help of the proposed method. This is due to the fact that using the classical method, the return period is calculated separately, for each sampled tree, using the age of the tree and the number of avalanches which left a mark on that particular tree. As a result, this method leads to an overestimation of the return period.

The number of reconstructed snow avalanches using the dendrogeomorphological method represents only approximately 40% of the snow avalanches which occurred in a particular avalanche path. Thus, the frequency of snow avalanches reconstructed with the help of the data taken from the tree rings represents only a minimum frequency (Luckman, 2010). Therefore, the result of applying the script presented in this study represents only a minimum number of avalanches produced in a particular avalanche path, leading to a maximum value of the return period.

Without using the interpolation, the return period calculated through the proposed method avoids unrealistic predictions which result from extrapolation (Johnston et al., 2001) in the areas located at a distance from the sampled trees, for example in the starting zone. However, a limitation of the proposed method can be noticed in the inferior part of the deposition or runout zone where there are no sampled trees and a recurrence interval cannot be determined.

A limitation of the proposed method was identified in the inferior sectors of the avalanche paths where the slopes are steeper than the path itself. In this situation, the upslope area algorithm marks the avalanche affected area on the path slopes, not inside the path. The aforementioned limitation is solved in most cases by applying the Delaunay triangulation before applying the upslope area algorithm.

5.3. The results of reconstructing the avalanche affected areas with the help of remote sensing

After calculating the 4 spectral indices (NBR, NDMI, MSI and DI) on the image from 29.07.1985 and the image from 18.09.1986, significant differences were noticed between the

two images. This is due to the destruction of the forested area as a consequence of avalanche occurrence.

In the case of the NBR index, the forested areas which recorded a decrease in the values which are higher than the established threshold are: the upper sector of the Zăvoaie path, both branches of this path, especially at their junction. In the entire alpine zone of the Parâng Mountains, significantly large areas where the destruction of the vegetation can be associated with snow avalanches were identified in other 13 avalanche paths. In the Scărița path, only a few pixels located near the upper limit of the forest suggest that an avalanche might have occurred in this area.

In the NDMI case, fewer pixels recorded larger decreases than the aforementioned threshold than in the previous case. In the entire alpine zone of the Parâng Mountains, clusters of affected pixels can be observed in the same paths as in the previous case. In the Zăvoaie path, each damaged tree has in its proximity at least one affected pixel. In the Scărița path, one notices only a few pixels which present significant decreases of the NDMI values.

In the MSI case, the forested areas affected by avalanches have recorded an increase of the values from 1986 in comparison to 1985. The areas which were highlighted by this index are larger than in the previous cases. In the Zăvoaie path, each tree which recorded the studied avalanche is inside or in the proximity of some affected pixels. However, in the Scărița path, only a few pixels recorded increases of the MSI values above the threshold.

In the DI case, the forested areas affected by avalanches also recorded an increase of their values. The areas which were highlighted by this index significantly differ from the areas identified with the previous indices. In the Zăvoaie path, the number of the affected pixels is smaller than in the previous cases. This kind of pixels are located in the upper part of the two path branches and in the inferior sector of the western branch. However, in the Scărița path, the areas which recorded an increase of the index values are concentrated in the upper part of this path. In the rest of the study area, the paths which were identified with the previous indices also present a concentration of the affected pixels.

In the avalanche paths located under the Păpușa Peak there were no identified pixels which would suggest the impact of avalanches on trees, because the Romanul path together with the neighboring area was covered by clouds in the image from 29 July 1985. In the Mușet path, this snow avalanche was not identified in the sampled trees.

After calculating the 4 spectral indices (NBR, NDMI, MSI and DI) on the images taken on 01.07.1984, 29.07.1985, 09.09.1986, 12.09.1987 and 05.08.1988, the spectral trajectory of the forested areas affected by avalanches was determined for each index. In the case of NBR,

the spectral trajectory highlights high values which are similar to the index from 1984 and 1985, followed by a sudden decrease in 1986, when the lowest values are recorded. Then, in 1987 and 1988 the values tend to increase, but they still do not reach the initial ones. In the areas outside the avalanche paths, the values of the index present only small variations.

In the NDMI case, the spectral trajectory highlights the same trend as in the case of the NBR. However, the decrease of the values recorded in 1986 in comparison to 1985 is more significant, reaching even negative values of the NDMI. The eventual increase of the values is slow and most of the pixels do not reach until 1988 the values recorded before the avalanche. In the areas outside the avalanche paths, the values of the index present only small variations.

In the MSI case, the spectral trajectory expresses a totally different trend. In the years 1984 and 1985, the values of the index are relatively low, but similar. In 1986, in the areas affected by avalanches, there is an increase of the values, in some pixels reaching the double of the value from 1985. In the following years, the values record a slight decrease, but in most of the pixels the initial values are no longer reached. In the areas outside the avalanche paths the values of the index present only small variations.

In the DI case, the spectral trajectory is similar to the MSI trajectory with lower initial values and a sudden increase in 1986. However, opposed to the MSI, after 1986, the values of the DI do not tend to decrease, but continue their increasing process in most of the affected pixels. Outside the avalanche paths, the DI values are much lower, presenting a clear dynamic: the highest value is recorded in 1988, the second value in 1984 and lower values between the two moments. The fact that after 1986 the DI values do not reach towards the initial values can be associated with this general dynamic which affects both the areas outside the avalanche paths and those inside them.

After the logistic regression was performed, out of the four variables which were included in this analysis, the highest score belonged to ΔDI (22.182), closely followed by ΔNBR (19.434). For ΔNDMI and ΔMSI, the score was significantly lower (2.275 and 2.911). The validity of the analysed correlation is confirmed by the results of the applied tests. The significance resulted from the Hosmer–Lemeshow test was 0.99. The Cox and Snell R^2 coefficient has the value 0.583. The Nagelkerke R^2 coefficient has the value 0.777.

The R^2 coefficients which resulted from the logistic regression are higher than 0.5. This confirms the fact that after the avalanche of 1986, the damage to the trees from the avalanche paths determined the spectral change of the paths, while in unaffected areas the spectral response remained the same.

5.4. Meteorological conditions required for the occurrence of snow avalanches

The regression analysis led to the identification of the meteorological conditions required for the occurrence of major avalanches, conditions that account for over 60% of the total variability ($R^2 = 0.676$).

The influence of each of the calculated meteorological parameters upon the activity of avalanches has been ranked according to the values of standardized beta coefficients. The main factor that leads to the occurrence of avalanches is the amount of precipitation fallen in April, irrespective of their aggregation state ($\beta = 0.432$). The parameter ranked second according to its relevance in triggering avalanches is the frequency of snow fall of 1 to 25 cm falling in 72h in January ($\beta = 0.415$). The third parameter is the daily average precipitation amount fallen in December ($\beta = 0.386$). The other relevant parameters for the occurrence of avalanches are: number of days in March with maximum temperature greater than the average maximum temperature plus the standard deviation ($\beta = -0.278$), average daily rainfall in February ($\beta = 0.245$), number of consecutive days with positive average temperature and snow cover in January ($\beta = 0.217$) as well as number of days in November when the snow measures 15 to 20 cm.

A winter with the highest occurrence probability of major snow avalanches would have to have the highest number of days with 15 cm to 20 cm of snow in November. The snowfall continues in December, but the snow layer has to increase slowly. The snow continues to pack in January, while increase in the snow cover alternates with warmer days. Snow melts during the day due to positive temperatures and freezes again during the night. Consequently, the snowpack is formed and ice sheets are embedded in the snow layers. In February snow continues to accumulate slowly without triggering instability to the snowpack. In March, the number of days with maximum temperatures exceeding the average plus the standard deviation must be as low as possible (β coefficient is negative). Considering the multiannual average maximum temperature of March of 10.3°C, temperatures exceeding this value frequently with more than one standard deviation trigger rapid thawing that results in reduced snowpack, insufficient for a major avalanche. Finally, new snowfall in April, although in reduced amount, will trigger major avalanches in the study area.

CONCLUSIONS

The thesis is a "classical" dendrogeomorphological reconstruction of avalanche activity performed for 4 avalanche paths in the alpine area of the Parâng Mountains. Based on growth anomalies visible in the collected tree samples, avalanches occurring in 34 winters in the last 100 years were identified.

The results confirm that this method can be successfully used in order to obtain information about former avalanches occurring in areas where evidence of avalanche activity is missing. This study improves the knowledge on past avalanche activity in the study area.

The avalanche in 1997 is the only one documented in the area due to its magnitude, especially in the western ridge extremities. This avalanche was reconstructed in 3 of the 4 analysed avalanche paths. In each case, it was of great magnitude, values of AAI coefficient exceeding 20%.

The customized formulas used in Microsoft Excel to centralize the growth anomalies identified in the sampled trees led to a smoother processing of this stage, as well as to a clearer picture of which of the sampled trees were impacted by the reconstructed avalanches. They also simplified the representation of growth anomalies in the graphs depicting the avalanche activity indices and facilitate the calculation of various statistics related to growth anomalies

The regional avalanche activity index indicates that the snow avalanches with the greatest impact at the study area scale were those that occurred in the winter of 2004-2005. A large number of avalanches occurred across the Carpathians that winter. Also, avalanches across all 4 avalanche paths were reconstructed for the winter of 2007-2008, but their magnitude was smaller (AAI of 15-19%). Avalanches occurring in 3 out of the 4 avalanche paths were reconstructed for the winters 1998-1999, 2002-2003 and 2011-2012.

The avalanche activity index, although introduced 30 years ago, is still relevant and useful as identification criteria for winters during which avalanches occurred. The 10% threshold that most researchers accept, facilitates the distinction between winters during which avalanches occurred and statistical noise. The “new” weighted avalanche activity index (Wit) has very nonuniform values between avalanche paths or for the same avalanche path when different years are considered. Because of the high value variation, no threshold could be set up for this index in order to be able to conclude that winters with a high value of Wit could have been winters during which avalanches occurred.

The correlation coefficients calculated for AAI and the distance covered by the snow avalanche, as well as the minimum altitude reached by the snow avalanche according to the location of the damaged trees have small values. Therefore, a longer distance covered by the snow avalanche or the fact that the avalanche reached a lower altitude are not necessarily reflected in a larger value of AAI. Similarly, snow avalanches that covered smaller distances or the fact that the snow avalanche stopped at a high altitude are not necessarily associated with smaller values of AAI.

For each reconstructed snow avalanche, the minimum extent was estimated automatically by assessing the relief features of the avalanche path and not by digitizing it manually as it was previously done.

Representing graphically and automatically the extent of the snow avalanche is part of an algorithm proposed for calculating the return period of these geomorphological processes. This algorithm has a new approach, the return period is no longer calculated for each sampled tree according to its age and snow avalanches that damaged the tree and also interpolation is no longer used. Its advantages include the possibility to estimate the return period inclusively in the starting zone, the fact that the estimated value is not influenced by the age of the sampled trees and it also takes the relief features into consideration.

The comparison of the return period values estimated with the proposed algorithm and the return period values estimated using the existing method outlines that the return period values are overestimated using the existing method. Trees growing in avalanche paths record only major snow avalanches that disturb their growth while minor snow avalanches cannot be captured in the chronologies reconstructed with the use of tree rings. Therefore, the shorter the return period, the closest to reality it its. Consequently, we conclude that the short return period values estimated using the proposed method reflect better the reality as opposed to the values estimated with the existing method.

The results of the reconstructions done in this study highlight an intense snow avalanche activity in the study area. In the upper section of the analysed avalanche paths their frequency if of one snow avalanche every 3 to 8 years. The frequency reduces along the path, in the lower section being of one snow avalanche every 14 to 30 years.

Besides the dendrogeomorphological reconstruction, the thesis presents a method to identify the extent of snow avalanches using satellite images. Combining the 2 methods confirms that by analysing 2 completely different types of data (tree rings and Landsat images), similar results regarding the extent of past snow avalanches can be obtained. Based on the results we can say that the two methods validate each other.

The analysis of meteorological conditions required to trigger major snow avalanches suggests that precipitation is the most important triggering factor. One important factor is the accumulation of snow all through the winter, as well as the instability of the snowpack in April as a result of new snowfall. Of great importance is the snow metamorphosis as well.

The studied snow avalanche paths are located in the proximity of Parâng and Transalpina ski areas. The presence of some valley areas covered in snow but not in forest can indicate to anyone the presence of an avalanche path. Therefore, the skiers skiing off track would be attracted to avalanche paths without being aware of the danger they expose themselves to due to the high frequency for snow avalanches in the upper sector of these avalanche paths.

The expansion of the Parâng ski area according to the plans approved by the Environmental Protection Agency in Hunedoara in 2011, implies the construction of ski infrastructure in the avalanche path in Scărița Valley as well as in the proximity of the avalanche path in Zăvoaie Valley. The implementation of this project should definitely take into consideration the intense activity of snow avalanches identified in these areas in order to not jeopardize the infrastructure and the lives of tourists using it.

The Transalpina road crosses the starting area of one of the most studied avalanche paths. This sector has been crossed by all 11 reconstructed avalanches. Besides some protection nets that should stop rock blocks from falling on the road there are no other protection elements that could protect the road from snow avalanche damages. Although the road is closed during winter, we consider that protection elements should be built in order to protect the road from the impact of the avalanches.

BIBLIOGRAPHY

Alestalo, J. (1971). Dendrochronological interpretation of geomorphic processes. *Fennia*.

Badea, L., Niculescu, G., Roată, S., Buza, M., & Sandu, M. (2001). *Unitățile de relief ale României* (Vol. 1 Carpații Meridionali și Munții Banatului). București: Editura Ars Docendi.

Birkeland, K. W., Mock, C. J., & Shinker, J. J. (2001). Avalanche extremes and atmospheric circulation patterns. *Annals of Glaciology, 32*, 135-140.

Bollschweiler, M., Stoffel, M., Schneuwly, D. M., & Bourqui, K. (2008). Traumatic resin ducts in Larix decidua stems impacted by debris flows. *Tree Physiology, 28*(2), 255-263.

Boucher, D., Filion, L., & Hétu, B. (2003). Reconstitution dendrochronologique et fréquence des grosses avalanches de neige dans un couloir subalpin du mont Hog's Back, en Gaspésie centrale (Québec). *Géographie physique et Quaternaire, 57*(2-3), 159-168.

Bud, M. (2008). *Ecoturismul în grupa montană Parâng.* București: Teză de doctorat, Facultatea de Geografie, Universitatea din București.

Cook, E. R., & Kairiukstis, L. A. (1992). *Methods of dendrochronology : applications in the environmental sciences.* Dordrecht: Kluwer Academic Publishers.

Coteț, P. (1973). *Geomorfologia României.* București: Editura Tehnică.

Cox, D. R., & Snell, E. J. (1989). *Analysis of binary data* (Vol. 32). CRC Press.

Dayton, C. M. (1992). Logistic regression analysis. *Stat*, 474-574.

Douglas, A. E. (1921). Dating our prehistoric ruins. *Natural History, 21*(1), 27-30.

Dragu, G., Dragomirescu, Ș., Oancea, D., Velcea, V. A., & Caloianu, N. (1987). *Geografia României. Vol. 3: Carpaţii Româneşti şi Depresiunea Transilvaniei.* București: Editura Academiei Republicii Socialiste România.

Du, S., & Yamamoto, F. (2007). An overview of the biology of reaction wood formation. *Journal of Integrative Plant Biology*, *49*(2), 131-143.

Fritts, H. C. (1976). *Tree Rings and Climate.* London: Academic Press.

Goodwin, N. R., Coops, N. C., Wulder, M. A., Gillanders, S., Schroeder, T. A., & Nelson, T. (2008). Estimation of insect infestation dynamics using a temporal sequence of Landsat data. *Remote Sensing of Environment, 112*(9), 3680-3689.

Healey, S. P., Cohen, W. B., Zhiqiang, Y., & Krankina, O. N. (2005). Comparison of Tasseled Cap-based Landsat data structures for use in forest disturbance detection. *Remote Sensing of Environment, 97*(3), 301-310.

Hosmer Jr, D. W., Lemeshow, S., & Sturdivant, R. X. (2013). *Applied logistic regression* (Vol. 398). John Wiley & Sons.

Iancu, S. (1970). *Muntii Parâng: studiu geomorfologic.* Cluj-Napoca: Teza de doctorat: Universitatea Babeș-Bolyai.

IBM. (2011). *IBM SPSS statistics for windows, version 22.0.* New York: IBM Corp Armonk.

Johnston, K., Ver Hoef, J. M., Krivoruchko, K., & Lucas, N. (2001). *Using ArcGIS geostatistical analyst* (Vol. 300). Redlands: ESRI.

Kauth, R. J., & Thomas, G. S. (1976). The tasselled cap--a graphic description of the spectral-temporal development of agricultural crops as seen by Landsat. *LARS Symposia* , 159.

Kennedy, R. E., Yang, Z., & Cohen, W. B. (2010). Detecting trends in forest disturbance and recovery using yearly Landsat time series: 1. LandTrendr—Temporal segmentation algorithms. *Sensing of Environment, 114*(2), 2897-2910.

Keylock, C. J. (2003). The North Atlantic oscillation and snow avalanching in Iceland. *Geophysical Research Letters, 30*(5).

Kogelnig-Mayer, B., Stoffel, M., Schneuwly-Bollschweiler, M., Hübl, J., & Rudolf-Miklau, F. (2011). Possibilities and limitations of dendrogeomorphic time-series reconstructions on sites influenced by debris flows and frequent snow avalanche activity. *Arctic, Antarctic, and Alpine Research, 43*(4), 649-658.

López García, M. J., & Caselles , V. (1991). Mapping burns and natural reforestation using Thematic Mapper data. *Geocarto International, 6*(1), 31-37.

Luckman, B. H. (2010). Dendrogeomorphology and Snow Avalanche Research. În M. Stoffel, M. Bollschweiler, D. R. Butler, & B. H. Luckman (Ed.), *Tree Rings and Natural Hazards* (pg. 27-34). Springer Netherlands.

Martonne, E. (1907). *Recherches sur l' évolution morphologique des Alpes de Transylvanie : (Karpates Méridionales).* Paris: Librairie Ch. Delagrave.

Masek, J. G., Vermote, E. F., Saleous, N. E., Wolfe, R., Hall, F. G., Huemmrich, K. F., Gao, F., Kutler, J., & Lim, T. (2006). A Landsat Surface Reflectance Dataset for North America, 1990–2000. *Geoscience and Remote Sensing Letters, IEEE, 3*(1), 68-72.

McClung, D., & Schaerer, P. (2006). *The Avalanche Handbook* (ed. 3rd). Seattle: The Mountaineers Books.

Meseșan, F., Gavrilă, I. G., & Pop, O. T. (2018a). Calculating snow-avalanche return period from tree-ring data. *Natural Hazards*. doi:https://doi.org/10.1007/s11069-018-3457-y

Meseșan, F., Man, T. C., Pop, O. T., & Gavrilă, I. G. (2018b). Reconstructing snow avalanche extent using remote sensing and dendrogeomorphology in Parâng Mountains. *Cold regions science and technology*. doi:https://doi.org/10.1016/j.coldregions.2018.10.002

Nagelkerke, N. J. (1991). A note on a general definition of the coefficient of determination. *Biometrika, 78*(3), 691-692.

Nagy, N. E., Franceschi, V. R., Solheim, H., Krekling, T., & Christiansen, E. (2000). Wound-induced traumatic resin duct development in stems of Norway spruce (Pinaceae): anatomy and cytochemical traits. *American Journal of Botany, 87*(3), 302-313.

Pop, O. T., Gavrilă, I. G., Roșian, G., Meseșan, F., Decaulne, A., Holobâcă, I. H., & Anghel, T. (2016). A century-long snow avalanche chronology reconstructed from tree-rings in Parâng Mountains (Southern Carpathians, Romania). *Quaternary International, 415*, 230-240.

Pop, O. T., Munteanu, A., Meseșan, F., Gavrilă, I. G., Timofte, C., & Holobâcă, I. H. (2018). Tree ring-based reconstruction of high-magnitude snow avalanches in Piatra Craiului Mountains (Southern Carpathians, Romania). *Geografiska Annaler: Series A, Physical Geography, 100*(2), 99-115.

Pop, O., Buimagă-Iarinca, S., Stoffel, M., & Anghel, T. (2012). Réponse des épicéas (Picea abies (L.) Karst.) à l'accumulation des sédiments dans le bassin de rétention Dumitrelul (Massif du Călimani, Roumanie). *Arbres et Dinamiques*, 71-88.

QGIS Development Team. (2016). QGIS geographic information system V. 2.18.

Reardon, B. A., Pederson, G. T., Caruso, C. J., & Fagre, D. B. (2008). Spatial reconstructions and comparisons of historic snow avalanche frequency and extent using tree rings in Glacier National Park, Montana, USA. *Arctic, Antarctic, and Alpine Research, 40*(1), 148-160.

RINNTECH. (2016). *RINNTECH - Technology for tree and wood analysis - LINTAB*. Preluat pe 03 23, 2018, de pe http://www.rinntech.de/content/view/16/47/lang,english/index.html

Rock, B. N., Williams, D. L., & Vogelmann, J. E. (1985). Field and airborne spectral characterization of suspected acid deposition damage in red spruce (Picea rubens) from Vermont. *Machine Processing of Remotely Sensed Data Symposium*, 71-81.

Săndulache, C. (2009). *Hazarde și riscuri naturale în Munții Parâng.* București: Teză de doctorat: Facultatea de Geografie, Universitatea din București.

Shroder, J. F. (1978). Dendrogeomorphological analysis of mass movement on Table Cliffs Plateau, Utah. *Quaternary Research, 9*(2), 168-185.

Simea, I. M. (2012). *Avalanșele din Munții Rodnei.* Cluj-Napoca: Teză de doctorat, Facultatea de Geografie,Universitatea Babeș Bolyai.

Stoffel, M., & Bollschweiler, M. (2008). Tree-ring analysis in natural hazards research – an overview. *Natural Hazards and Earth System Sciences, 8*, 187–202.

Stoffel, M., & Bollschweiler, M. (2009). What Tree Rings Can Tell About Earth-Surface Processes: Teaching the Principles of Dendrogeomorphology. *Geography Compass, 3*(3), 1013-1037.

Stoffel, M., & Corona, C. (2014). Dendroecological dating of geomorphic disturbance in trees. *Tree-Ring Research, 70*(1), 3-20.

Stoffel, M., Butler, D. R., & Corona, C. (2013). Mass movements and tree rings: A guide to dendrogeomorphic field sampling and dating. *Geomorphology, 200,* 106-120.

Wenk, C. (1999). Applying an edit distance to the matching of tree ring sequences in dendrochronology. În M. Crochemore, & M. Paterson (Ed.), *Combinatorial Pattern Matching* (pg. 223-242). Berlin Heidelberg: Springer.